

Quantum algorithms for dynamics and dynamical observables

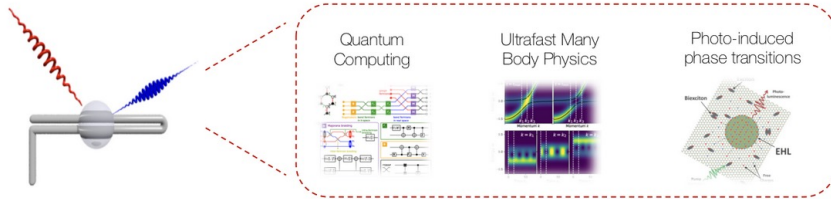
Alexander (Lex) Kemper



Department of Physics
North Carolina State University
<https://go.ncsu.edu/kemper-lab>

Virginia Tech
11/16/2023





Kemper Lab

Quantum materials in and out of equilibrium.

Collaborations with:

- Bojko Bakalov (NCSU)
- Marco Cerezo, Martin de la Rocca (LANL)
- Jim Freericks (Georgetown)
- Daan Camps, Roel van Beeumen, Bert de Jong, Akhil Francis (LBNL)
- Thomas Steckmann (UMD)
- Yan Wang, Eugene Dumitrescu (ORNL)

Current members



Alexander (Lex) Kemper
Principal investigator



Efehan Kökcü
Graduate Researcher



Anjali Agrawal
Graduate Researcher



Heba Labib
Graduate Researcher



Jack Howard
Undergraduate Researcher



Natalia Wilson
Undergraduate Researcher



Daniel Brandon
Undergraduate Researcher



Sarah Klas
Undergraduate Researcher



Norman Hogan
Graduate Researcher



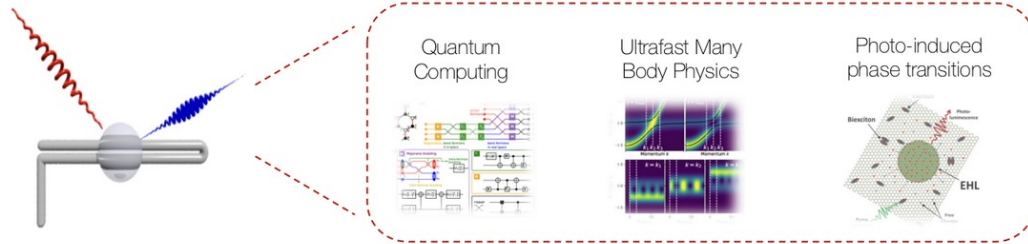
Ethan Blair
Undergraduate Researcher



Your Name
New lab member

- Quantum Matter meets Quantum Computing
- Response functions
 - Why we care
 - How do find them
- A different paradigm: Making the experiment part of the simulation via linear response
- Lie algebras for fun and profit (and quantum computing)

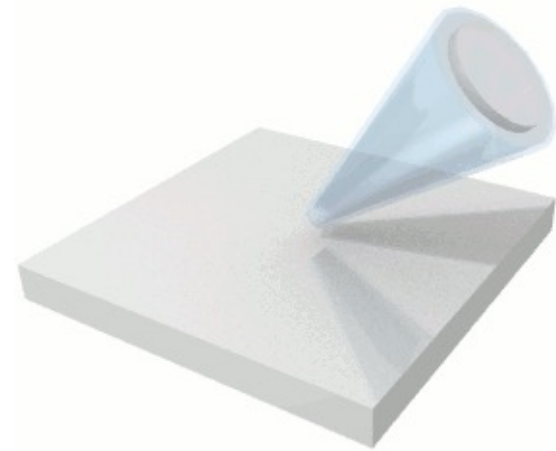
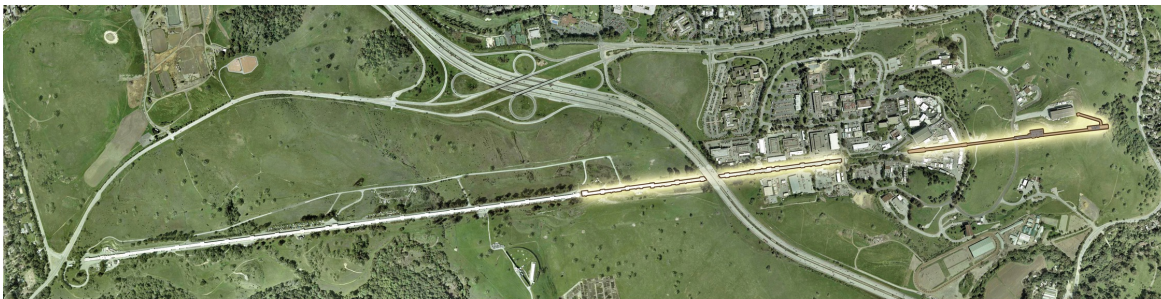
Why quantum computing for condensed matter?



Kemper Lab

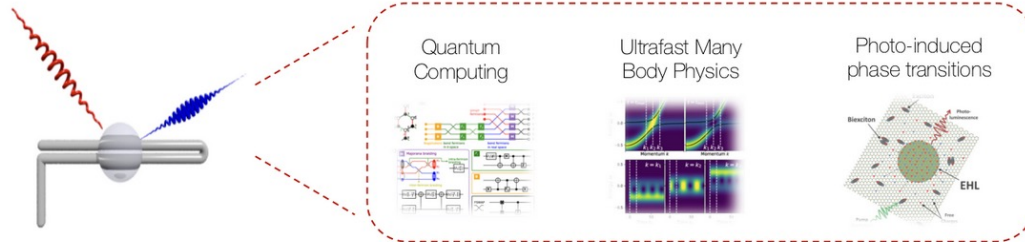
Quantum materials in and out of equilibrium.

Time-resolved experiments



Shen group (Stanford)

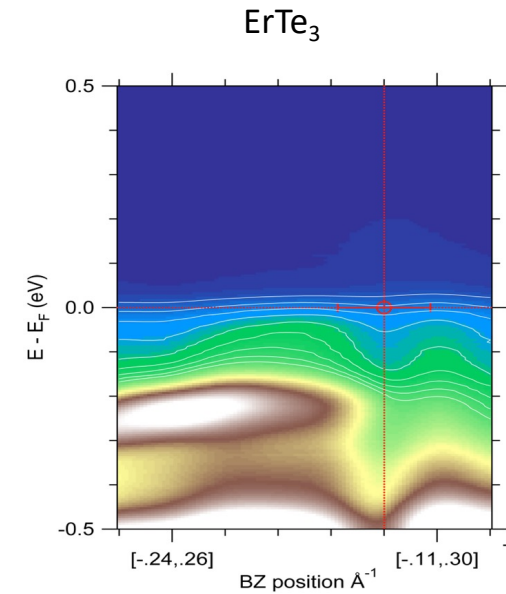
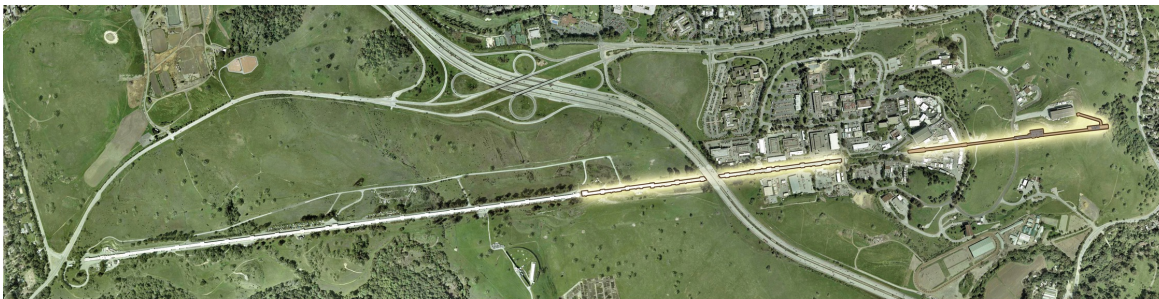
Why quantum computing for condensed matter?



Kemper Lab

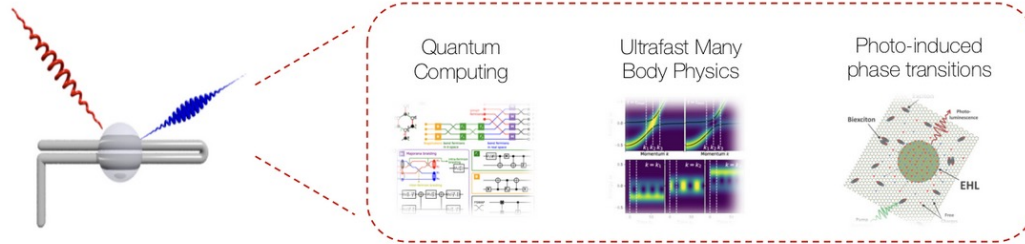
Quantum materials in and out of equilibrium.

Time-resolved experiments



Shen group (Stanford)

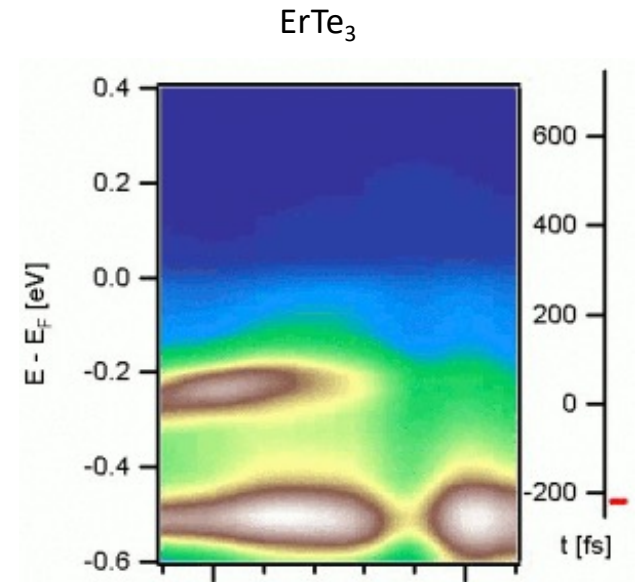
Why quantum computing for condensed matter?



Kemper Lab

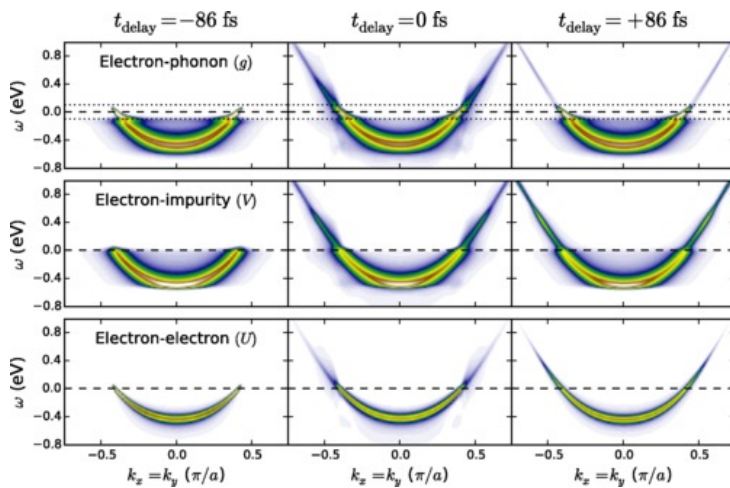
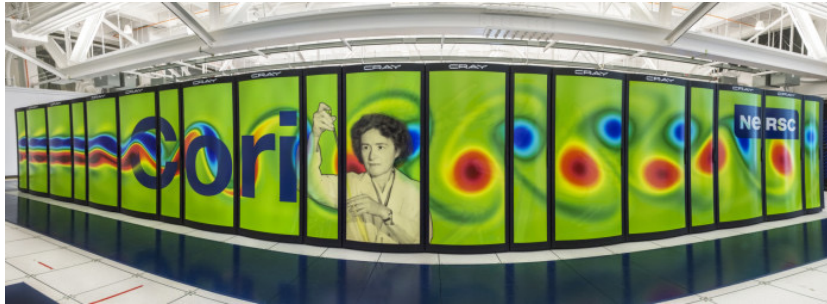
Quantum materials in and out of equilibrium.

Time-resolved experiments

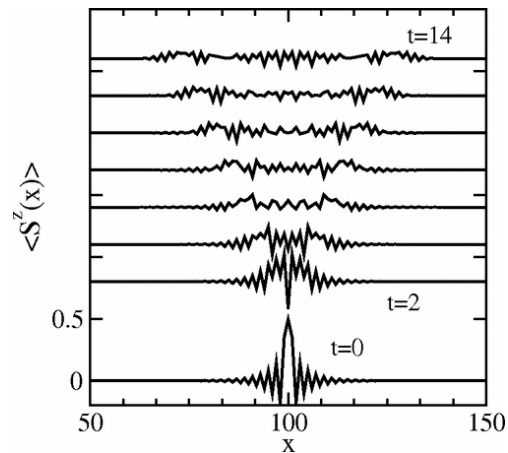


Shen group (Stanford)

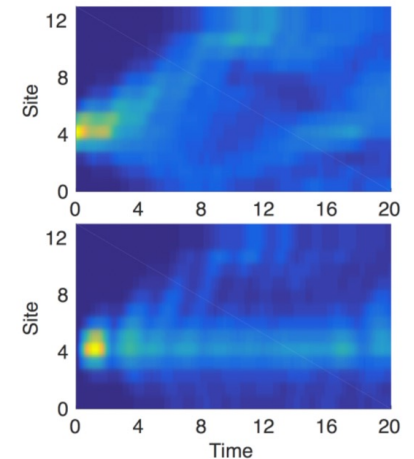
Why quantum computing for condensed matter?



Non-Equilibrium Green's functions
Phys. Rev. X 8, 041009 (2018)



Time domain DMRG
Phys. Rev. Lett. 93, 076401 (2004)

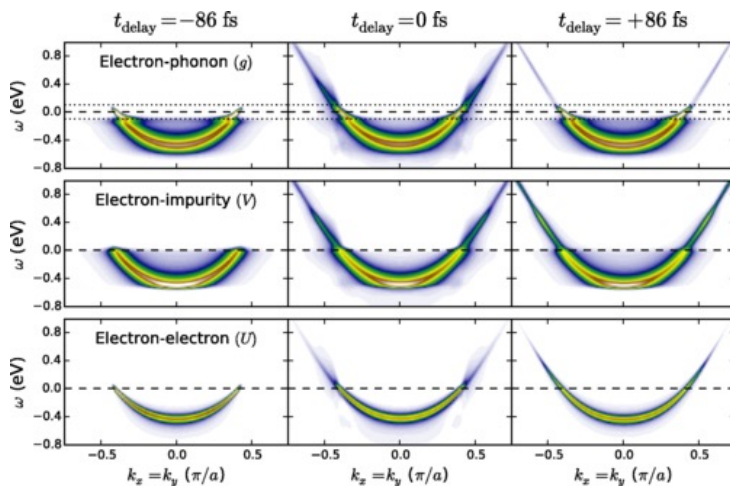


Time domain ED
Johnston & Kemper, unpublished

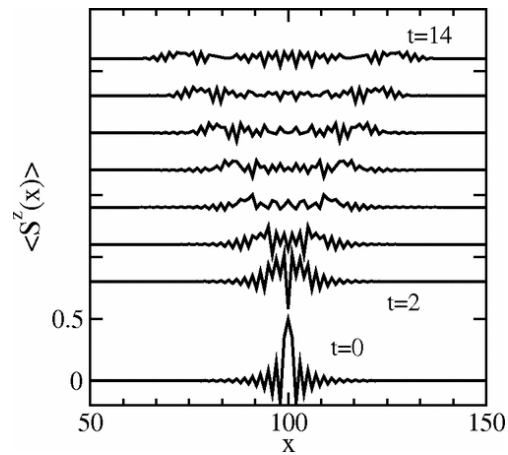
Why quantum computing for condensed matter?



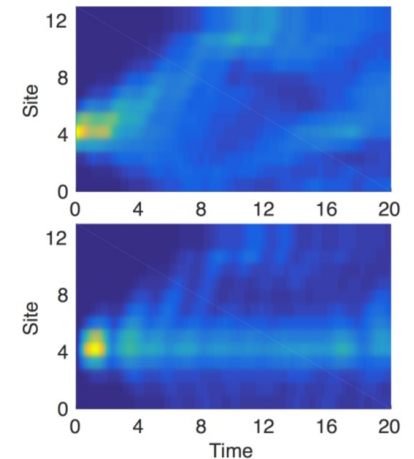
All these techniques eventually reach a barrier.



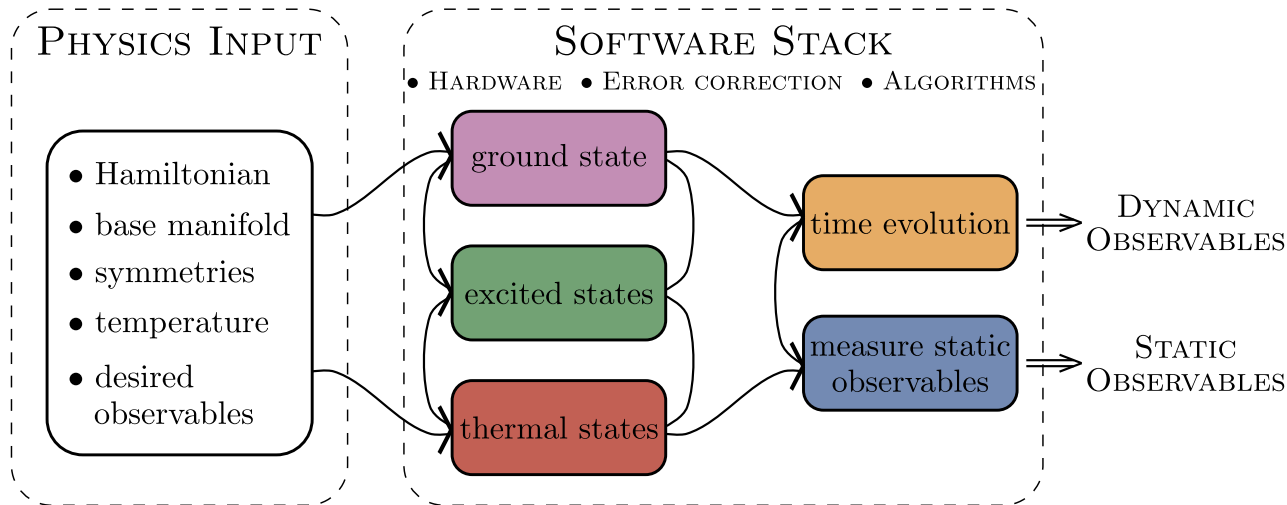
Non-Equilibrium Green's functions
Phys. Rev. X 8, 041009 (2018)



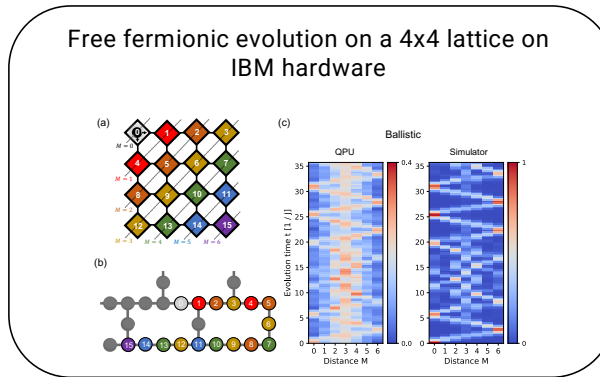
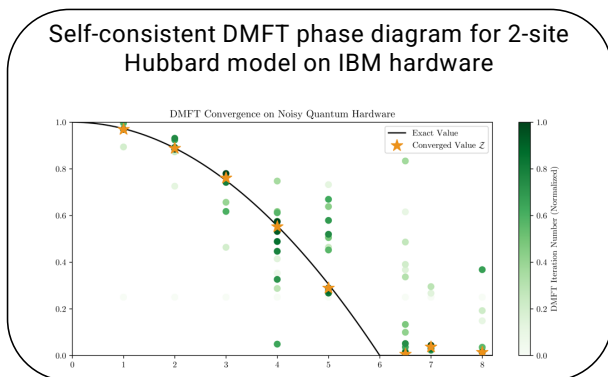
Time domain DMRG
Phys. Rev. Lett. 93, 076401 (2004)



Time domain ED
Johnston & Kemper, unpublished



- **Experimental relevance: Measuring correlation functions**
- Measuring exact integer Chern numbers for topological states
- Driven/dissipative systems and fixed points (1000 Trotter steps)



- **Exact time evolution via Lie algebraic decomposition and compression**
- Thermodynamics via Lee-Yang Zeros
- Physics-Informed Subspace Expansions

Q: What do you do with a quantum state once you've prepared one?

Ising Model

794

Brazilian Journal of Physics, vol. 30, no. 4, December, 2000

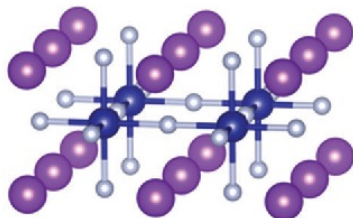
The Ising Model and Real Magnetic Materials

W. P. Wolf

Yale University, Department of Applied Physics,
P.O. Box 208284, New Haven, Connecticut 06520-8284, U.S.A.

Received on 3 August, 2000

The factors that make certain magnetic materials behave similarly to corresponding Ising models are reviewed. Examples of extensively studied materials include $\text{Dy}(\text{C}_2\text{H}_3\text{SO}_4)_3 \cdot 9\text{H}_2\text{O}$ (DyES), $\text{Dy}_2\text{Al}_2\text{O}_7$ (DyAlG), DyPO_4 , $\text{Dy}_2\text{Ti}_2\text{O}_7$, LiTbF_4 , K_2CoF_4 , and Rb_2CoF_4 . Various comparisons between theory and experiment for these materials are examined. The agreement is found to be generally very good, even when there are clear differences between the ideal Ising model and the real materials. In a number of experiments behavior has been observed that requires extensions of the usual Ising model. These include the effects of long range magnetic dipole interactions, competing interaction effects in field-induced phase transitions, induced staggered field effects and frustration effects, and dynamic effects. The results show that the Ising model and real magnetic materials have provided an unusually rich and productive field for the interaction between theory and experiment over the past 40 years.



[10.1039/c6cp02362b](https://doi.org/10.1039/c6cp02362b)

Heisenberg model

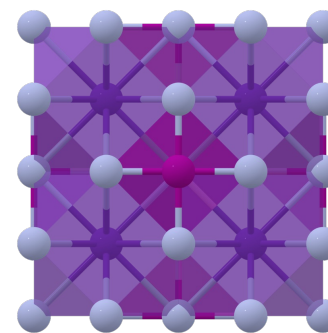
PHYSICAL REVIEW B

covering condensed matter and materials physics

Highlights Recent Accepted Collections Authors Referees Search Press

Critical behavior of the three-dimensional Heisenberg antiferromagnet RbMnF_3

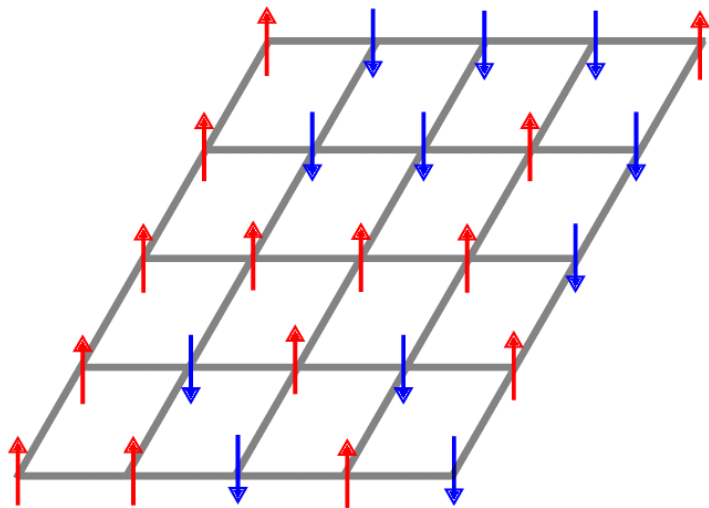
R. Coldea, R. A. Cowley, T. G. Perring, D. F. McMorrow, and B. Roessli
Phys. Rev. B **57**, 5281 – Published 1 March 1998



Materials project

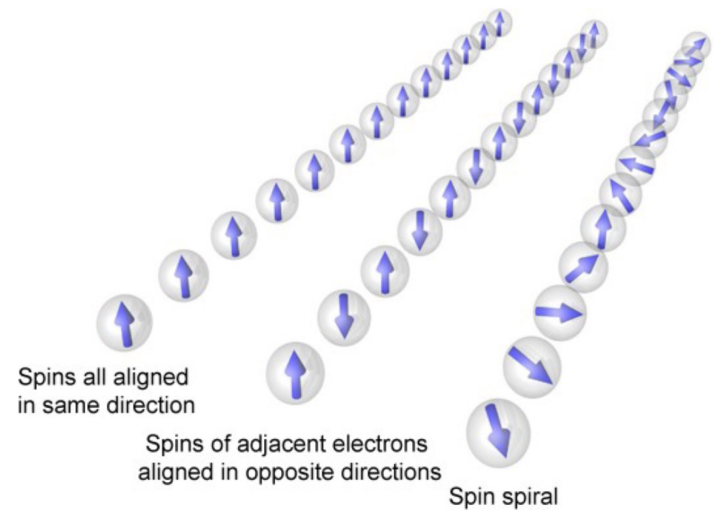
Ising Model

$$\mathcal{H} = -J \sum_i \sigma_i^z \sigma_{i+1}^z + h_x \sum_i \sigma_i^x$$



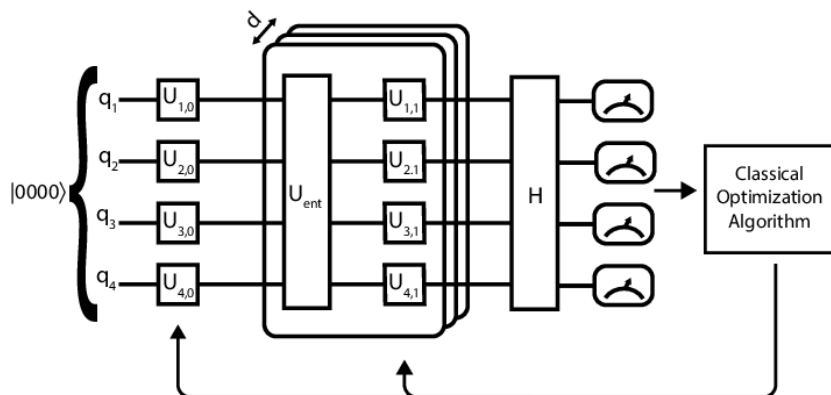
Heisenberg model

$$\mathcal{H} = -J \sum_i \vec{\sigma}_i \cdot \vec{\sigma}_{i+1} + h_x \sum_i \sigma_i^x$$



Ising Model

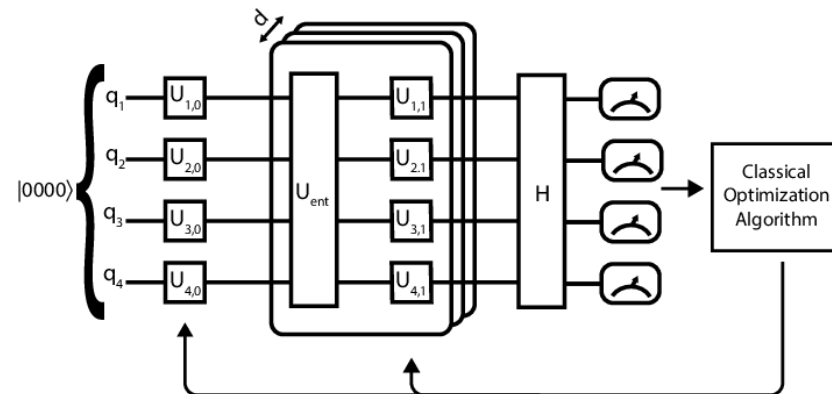
$$\mathcal{H} = -J \sum_i \sigma_i^z \sigma_{i+1}^z + h_x \sum_i \sigma_i^x$$



[Optimization of the Variational Quantum Eigensolver for Quantum Chemistry Applications](#)

Heisenberg model

$$\mathcal{H} = -J \sum_i \vec{\sigma}_i \cdot \vec{\sigma}_{i+1} + h_x \sum_i \sigma_i^x$$



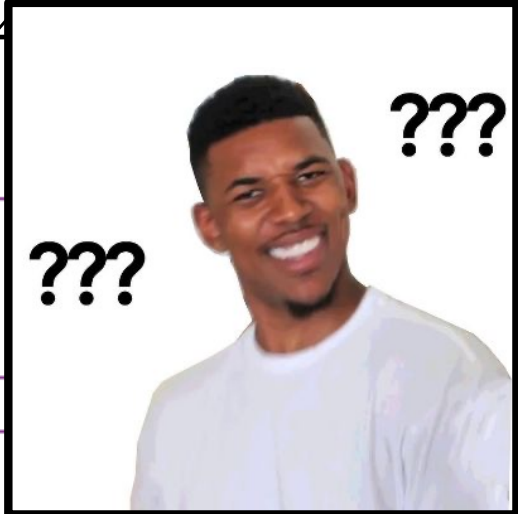
Ising Model

$$\mathcal{H} = -J \sum_i \sigma_i^z \sigma_{i+1}^z + h_x \sum_i \sigma_i^x$$

Ferromagnetic



Antiferromagnetic



Heisenberg model

$$\mathcal{H} = -J \sum_i \vec{\sigma}_i \cdot \vec{\sigma}_{i+1} + h_x \sum_i \sigma_i^x$$

Ferromagnetic



Antiferromagnetic



Ising Model

794

Brazilian Journal of Physics, vol. 30, no. 4, December, 2000

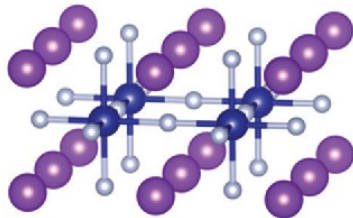
The Ising Model and Real Magnetic Materials

W. P. Wolf

Yale University, Department of Applied Physics,
P.O. Box 208284, New Haven, Connecticut 06520-8284, U.S.A.

Received on 3 August, 2000

The factors that make certain magnetic materials behave similarly to corresponding Ising models are reviewed. Examples of extensively studied materials include $\text{Dy}(\text{C}_2\text{H}_3\text{SO}_4)_2$, $\text{Dy}_3\text{Al}_5\text{O}_{12}$ (DyAlG), DyPO_4 , $\text{Dy}_2\text{Ti}_2\text{O}_7$, LiTbF_4 , K_2CoF_4 , and Rb_2CoF_4 . Variations between theory and experiment for these materials are examined. The agreement is generally very good, even when there are clear differences between the ideal Ising model and real materials. In a number of experiments behavior has been observed that requires a generalization of the usual Ising model. These include the effects of long range magnetic dipole interactions, anisotropy, interaction effects in field-induced phase transitions, induced staggered field effects, and dynamic effects. The results show that the Ising model and real magnetic materials have provided an unusually rich and productive field for the interaction between theory and experiment over the past 40 years.



[10.1039/c6cp02362b](https://doi.org/10.1039/c6cp02362b)

Heisenberg model

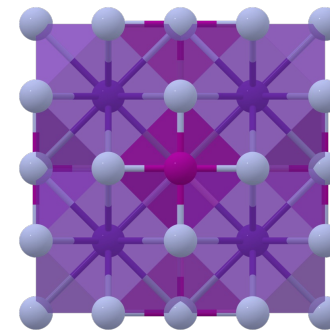
PHYSICAL REVIEW B

Condensed matter and materials physics

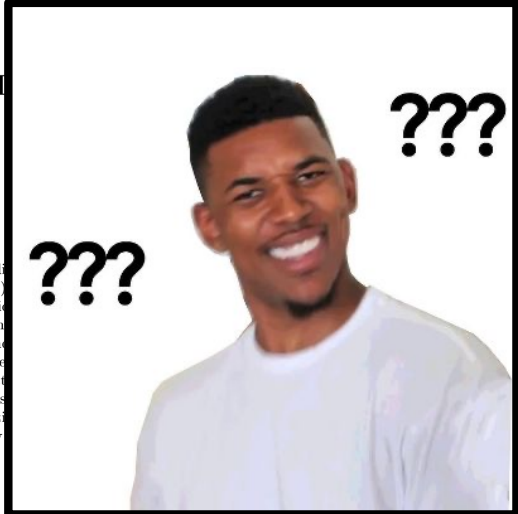
Recent Accepted Collections Authors Referees Search Press

Magnetic behavior of the three-dimensional Heisenberg ferromagnet RbMnF_3

by R. A. Cowley, T. G. Perring, D. F. McMorrow, and B. Roessli
Phys. Rev. B **57**, 5281 – Published 1 March 1998



Materials project

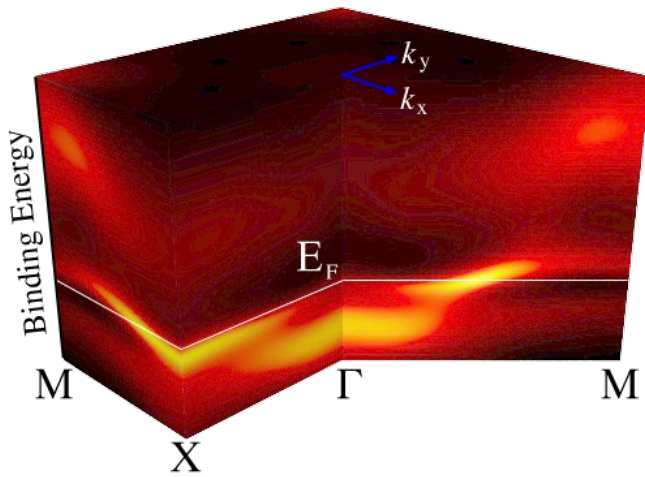


Q: What do you do with a quantum state once you've prepared one?

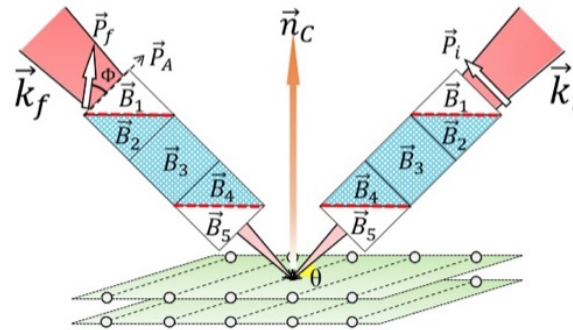
A: You measure its excitations.

Measuring Excitations

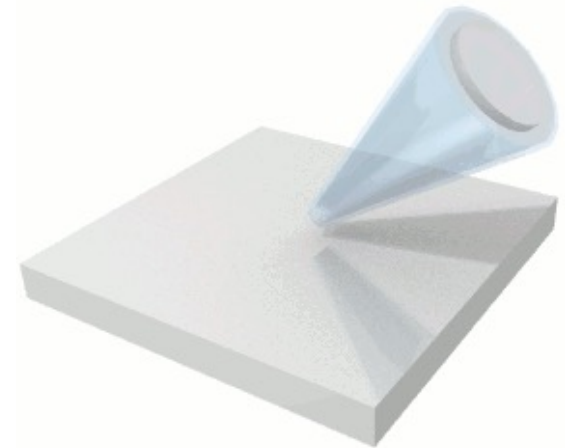
Figures courtesy of
Devereaux/Shen group
and ORNL



Angle-resolved Photoemission
(ARPES)

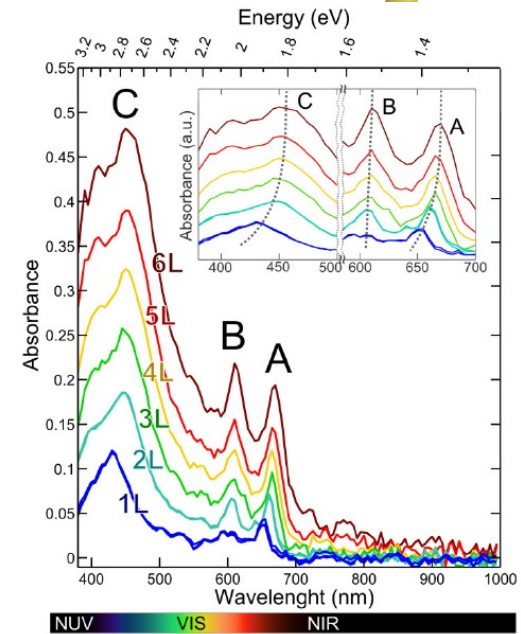
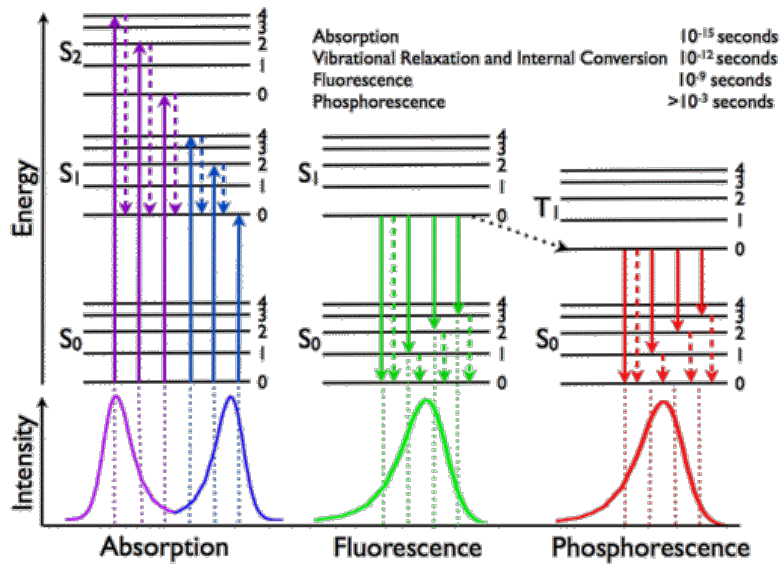
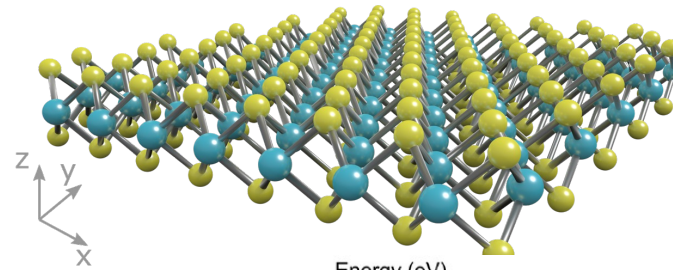
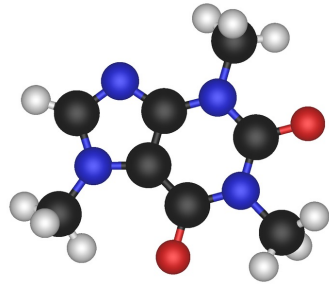


Neutron Scattering



Time-resolved ARPES

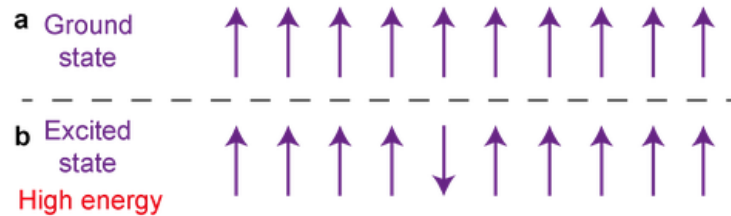
Measuring Excitations



Measuring Excitations

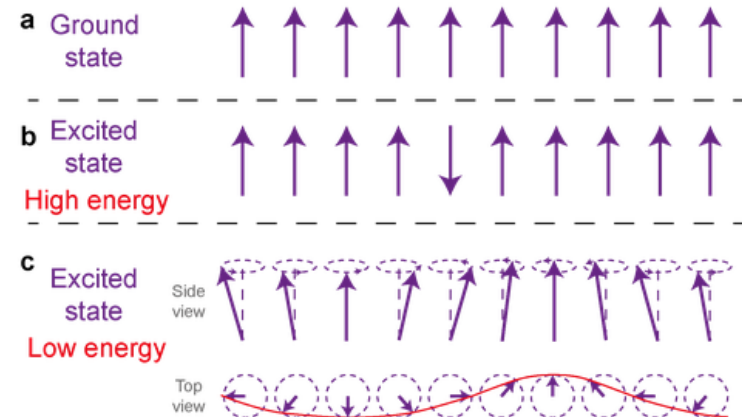
Ising Model

$$\mathcal{H} = -J \sum_i \sigma_i^z \sigma_{i+1}^z + h_x \sum_i \sigma_i^x$$

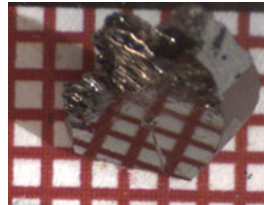


Heisenberg model

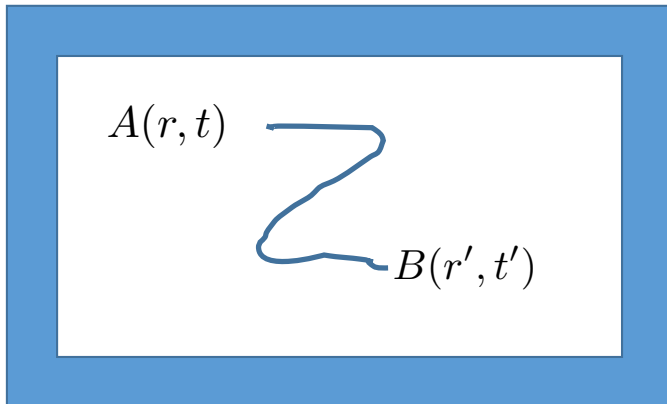
$$\mathcal{H} = -J \sum_i \vec{\sigma}_i \cdot \vec{\sigma}_{i+1} + h_x \sum_i \sigma_i^x$$



Correlation functions



$$\langle A(r, t) B(r', t') \rangle$$



Given some (observable) operator B at (r', t') , what is the likelihood of some (observable) operator A at (r, t) ?

Optical conductivity, γ /X-ray scattering, photoemission, neutron scattering, Raman, IR absorption, etc.

$$\delta A(t) = -i \int_{-\infty}^t \langle [\mathbf{A}(t), \mathbf{B}] \rangle h(\bar{t}) d\bar{t} = \int_{-\infty}^{\infty} \chi^R(t, \bar{t}) h(\bar{t}) d\bar{t}$$

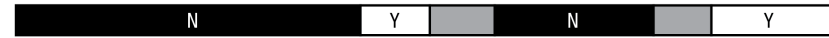
Experiment	Applied field B	Measured operator A	Correlation function
AC Conductivity	Electric field	Current	[j,j]
Neutron Scattering	Spin flip	Spin flip/Z	[Sx,Sx] etc
Magnetic Susceptibility	Magnetic	Spin	[Sz,Sz], [S+,S-]
Photoemission spectroscopy	Particle removal	Particles at detector	[c ⁺ c]
Light absorption	p.A	j	A.[p, j]
Light scattering	p.A	p.A	A1.[p1, p2].A2

$$\delta A(t) = -i \int_{-\infty}^t \langle [\mathbf{A}(t), \mathbf{B}] \rangle h(\bar{t}) d\bar{t} = \int_{-\infty}^{\infty} \chi^R(t, \bar{t}) h(\bar{t}) d\bar{t}$$

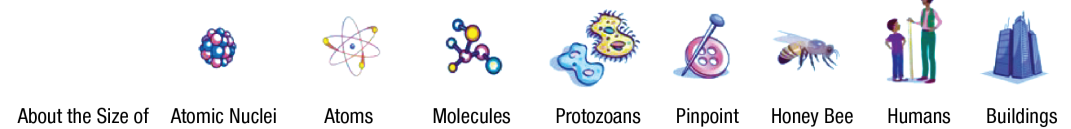
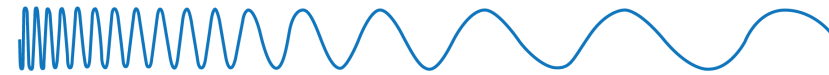


THE ELECTROMAGNETIC SPECTRUM

Penetrate Earth's Atmosphere



Radiation Type	Gamma Ray	X-ray	Ultraviolet	Visible	Infrared	Microwave	Radio
Wavelength (m)	10^{-12}	10^{-10}	10^{-8}	5×10^{-6}	10^{-5}	10^{-1}	10^3

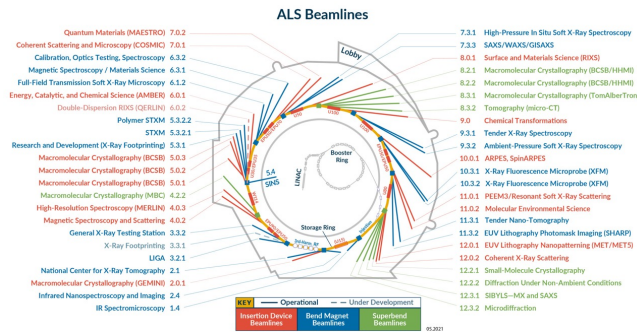


Short wavelength
High energy
High frequency

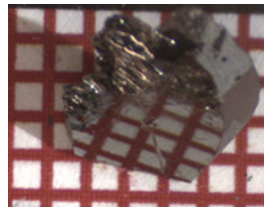
Long wavelength
Low energy
Low frequency



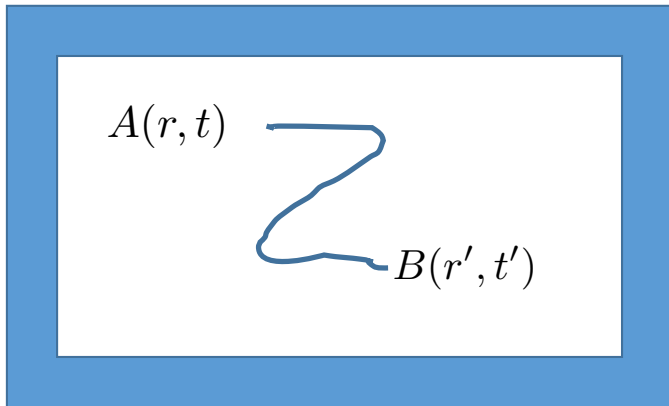
The Electromagnetic Spectrum. Image Credit: NASA



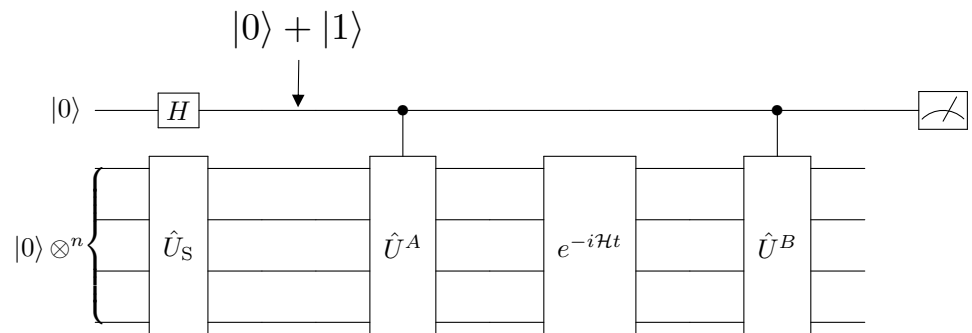
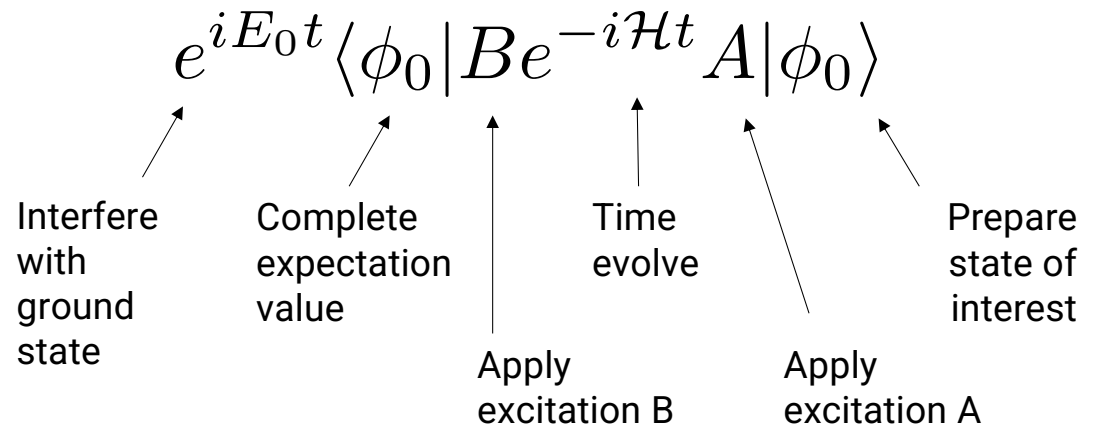
Correlation functions



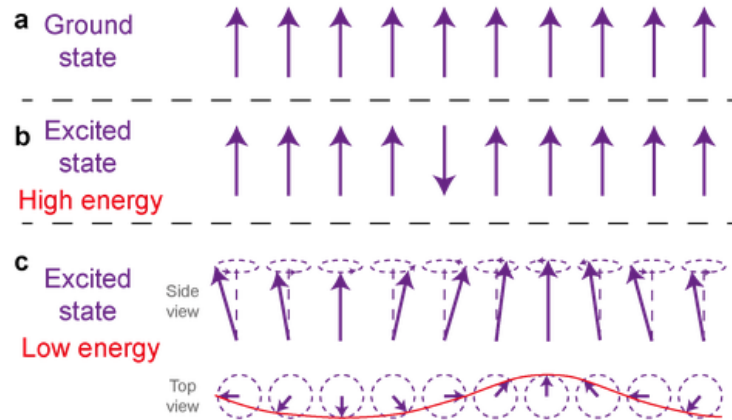
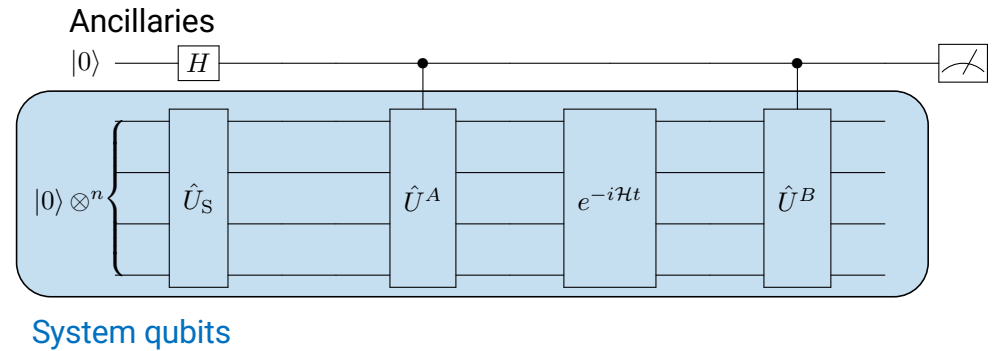
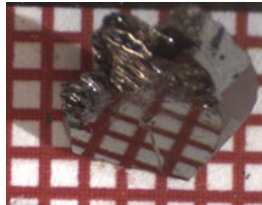
Interfere with ground state



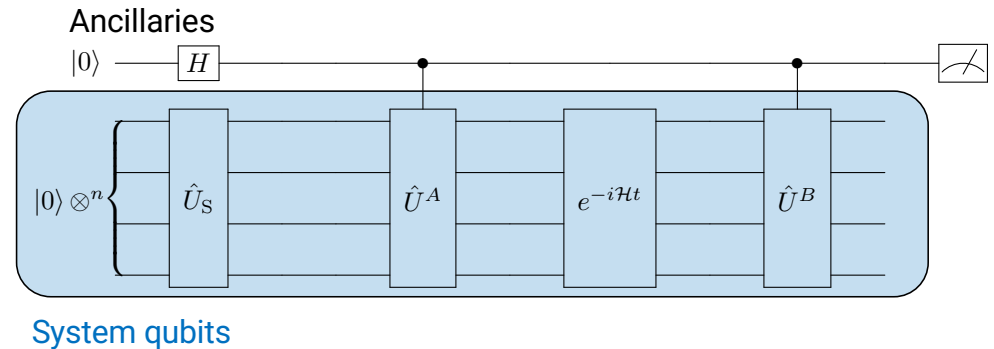
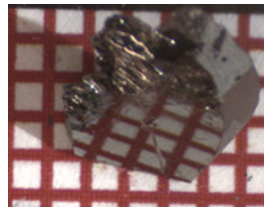
Somma, *Simulating physical phenomena by quantum networks* (2002)



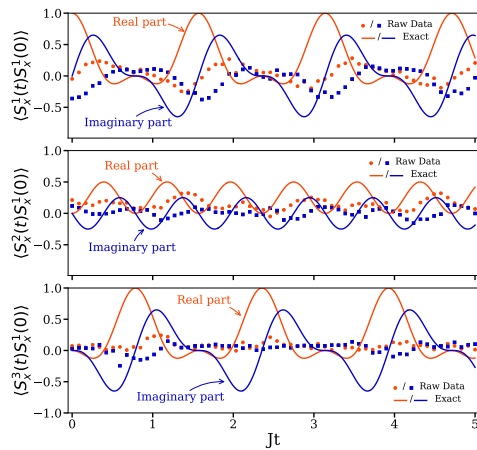
Correlation functions



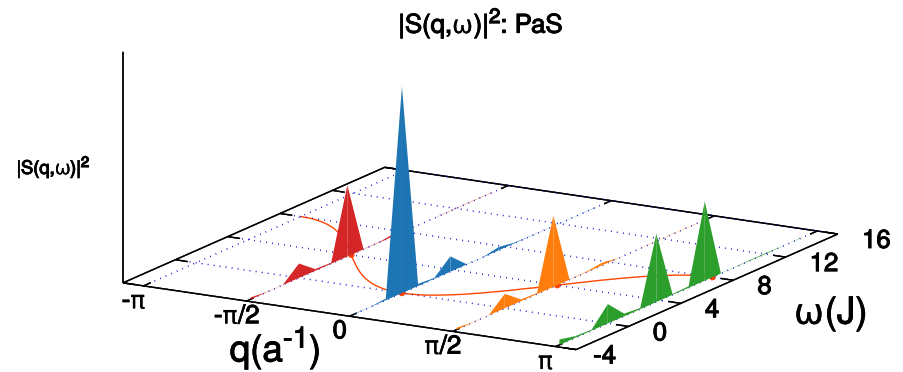
Correlation functions



Raw data (2019)

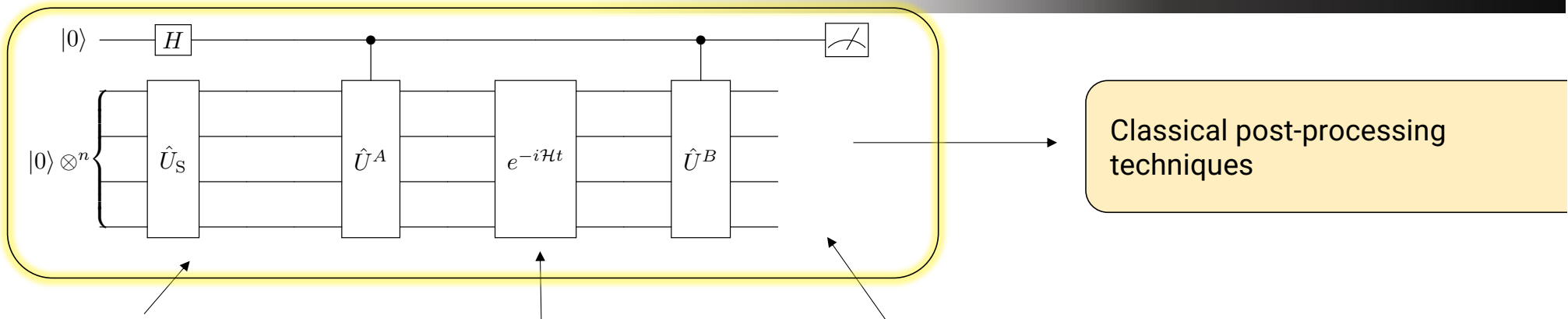


Error mitigation



$$\langle A(r, t) B(r', t') \rangle$$

A-Z quantum simulation



Prepare state of interest

Time evolve

Dynamical response functions

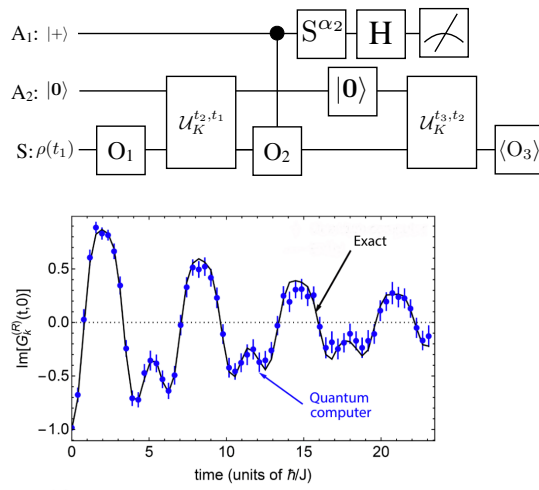
- *Physics-Informed Subspace Expansions*

- *Lie-algebraic methods for time evolution*
- *Open quantum system evolution*

- *Neutron scattering (magnon) spectra*
- *Open quantum system Green's functions*
- *Dynamical Mean Field Theory*

Robust measurements of n-point correlation functions of driven-dissipative quantum systems on a digital quantum computer

Lorenzo Del Re,^{1,2} Brian Rost,¹ Michael Foss-Feig,³ A. F. Kemper,⁴ and J. K. Freericks¹
¹Department of Physics, Georgetown University, 37th and O Sts., NW, Washington, DC 20057, USA
²Max Planck Institute for Solid State Research, D-70569 Stuttgart, Germany
³Quantinuum, 303 S. Technology Ct, Broomfield, Colorado 80021, USA
⁴Department of Physics, North Carolina State University, Raleigh, North Carolina 27695, USA
 (Dated: April 27, 2022)



(Anti-)Commutators, open/dissipative

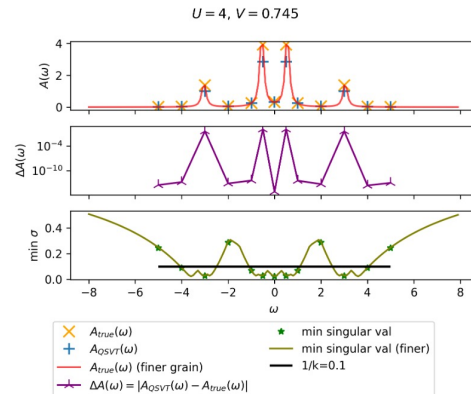
L. Del Re, B. Rost, M. Foss-Feig, AFK, J.K. Freericks
 2204.12400

Quantum Computed Green's Functions using a Cumulant Expansion of the Lanczos Method

Gabriel Greene-Diniz,^{1,*} David Zsolt Manrique,¹ Kentaro Yamamoto,² Evgeny Plekhanov,¹ Nathan Fitzpatrick,¹ Michal Krompiec,¹ Rei Sakuma,³ and David Muñoz Ramo¹
¹Quantinuum, Terrington House, 13-15 Hills Road, Cambridge CB2 1NL, UK
²Quantinuum K.K., Otemachi Financial City Grand Cube SF, 1-9-2 Otemachi, Chiyoda-ku, Tokyo, Japan
³Materials Informatics Initiative, RD Technology & Digital Transformation Center, JSR Corporation, 3-103-9, Tonomachi, Kawasaki-shi, Kawasaki, 210-0821, Kanagawa, Japan.
 (Dated: September 19, 2023)

Calculating the Single-Particle Many-body Green's Functions via the Quantum Singular Value Transform Algorithm

Alexis Ralli,^{1,2,*} Gabriel Greene-Diniz,¹ David Muñoz Ramo,¹ and Nathan Fitzpatrick^{1,†}
¹Quantinuum, 13-15 Hills Road, CB2 1NL, Cambridge, United Kingdom
²Centre for Computational Science, Department of Chemistry, University College London, WC1H 0AJ, United Kingdom
 (Dated: July 26, 2023)



Probing Real-Space and Time-Resolved Correlation Functions with Many-Body Ramsey Interferometry

Michael Knap,^{1,2,*} Adrian Kantian,³ Thierry Giamarchi,³ Immanuel Bloch,^{4,5} Mikhail D. Lukin,¹ and Eugene Demler¹
¹Department of Physics, Harvard University, Cambridge, Massachusetts 02138, USA
²ITAMP, Harvard-Smithsonian Center for Astrophysics, Cambridge, Massachusetts 02138, USA
³DPMC-MaNEP, University of Geneva, 24 Quai Ernest-Ansermet CH-1211 Geneva, Switzerland
⁴Max-Planck-Institut für Quantenoptik, Hans-Kopfermann-Straße 1, 85748 Garching, Germany
⁵Fakultät für Physik, Ludwig-Maximilians-Universität München, 80799 München, Germany
 (Received 2 July 2013; revised manuscript received 18 September 2013; published 4 October 2013)

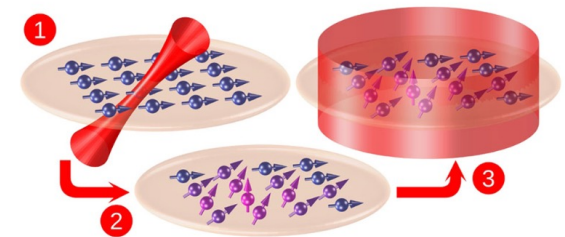
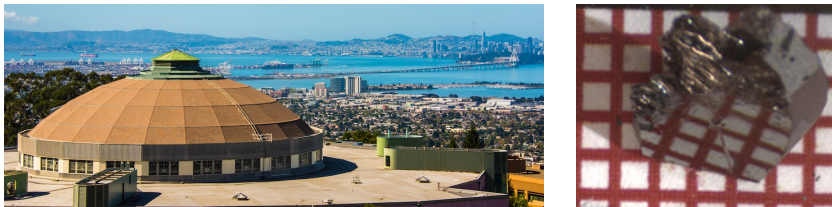


FIG. 1 (color online). Many-body Ramsey interferometry consists of the following steps: (1) A spin system prepared in its ground state is locally excited by $\pi/2$ rotation; (2) the system evolves in time; (3) a global $\pi/2$ rotation is applied, followed by the measurement of the spin state. This protocol provides the dynamic many-body Green's function.

Commutators

10.1103/PhysRevLett.111.147205



A linear response framework for simulating bosonic and fermionic correlation functions illustrated on quantum computers

Efekan Kökcü ¹, Heba A. Labib ¹, J. K. Freericks ², and A. F. Kemper ^{1,*}

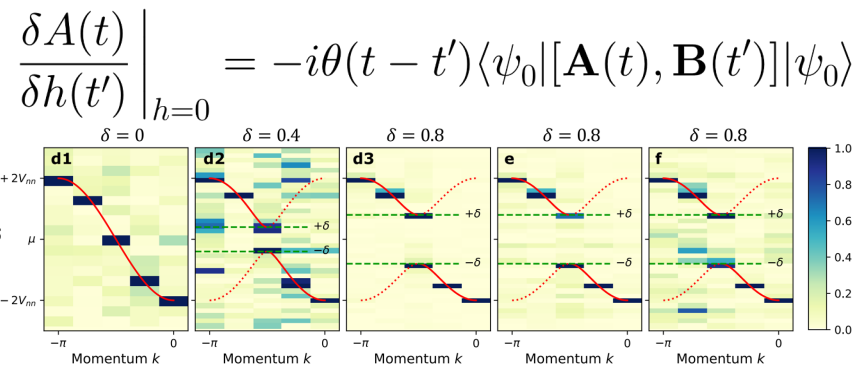
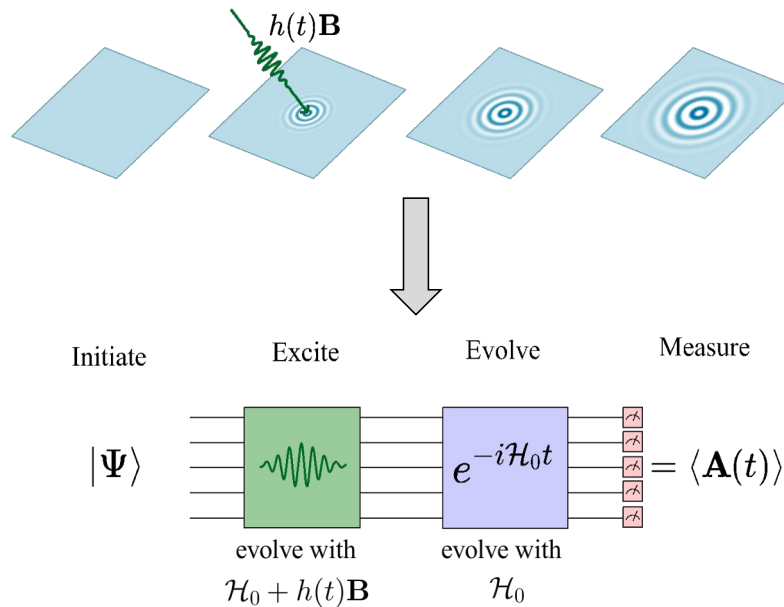
¹Department of Physics, North Carolina State University, Raleigh, North Carolina 27695, USA

²Department of Physics, Georgetown University, 37th and O Sts. NW, Washington, DC 20057 USA

(Dated: February 22, 2023)





1. Make the excitation part of the quantum simulation

2. Post-process the data to get the response functions





A linear response framework for simulating bosonic and fermionic correlation functions illustrated on quantum computers

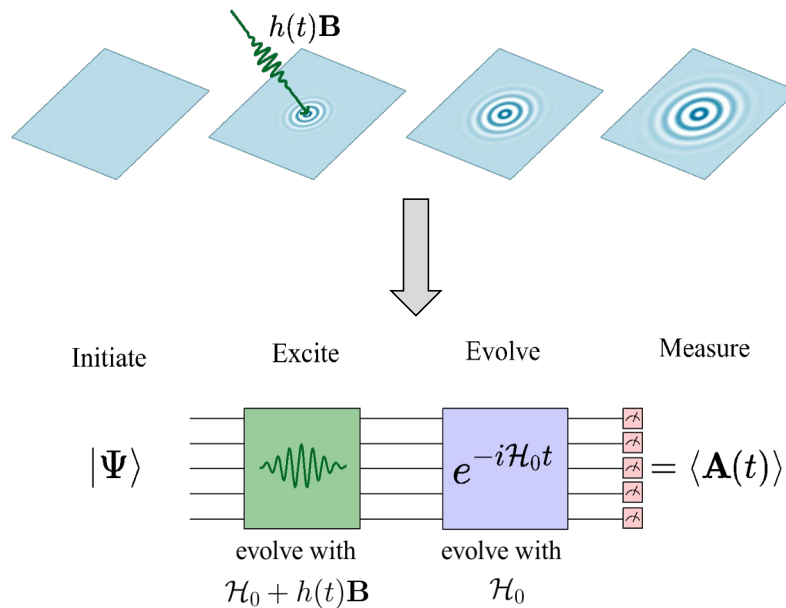
Efekan Kökcü ¹, Heba A. Labib ¹, J. K. Freericks ² and A. F. Kemper ^{1,*}

¹Department of Physics, North Carolina State University, Raleigh, North Carolina 27695, USA

²Department of Physics, Georgetown University, 37th and O Sts. NW, Washington, DC 20057 USA
(Dated: February 22, 2023)

Benefits

- Any operator A,B you desire (as long as it is Hermitian*)
- No ancillas/controlled operations needed
- Many correlation functions at the same time
- Less post-processing (less noise)
- Frequency/momentum selective

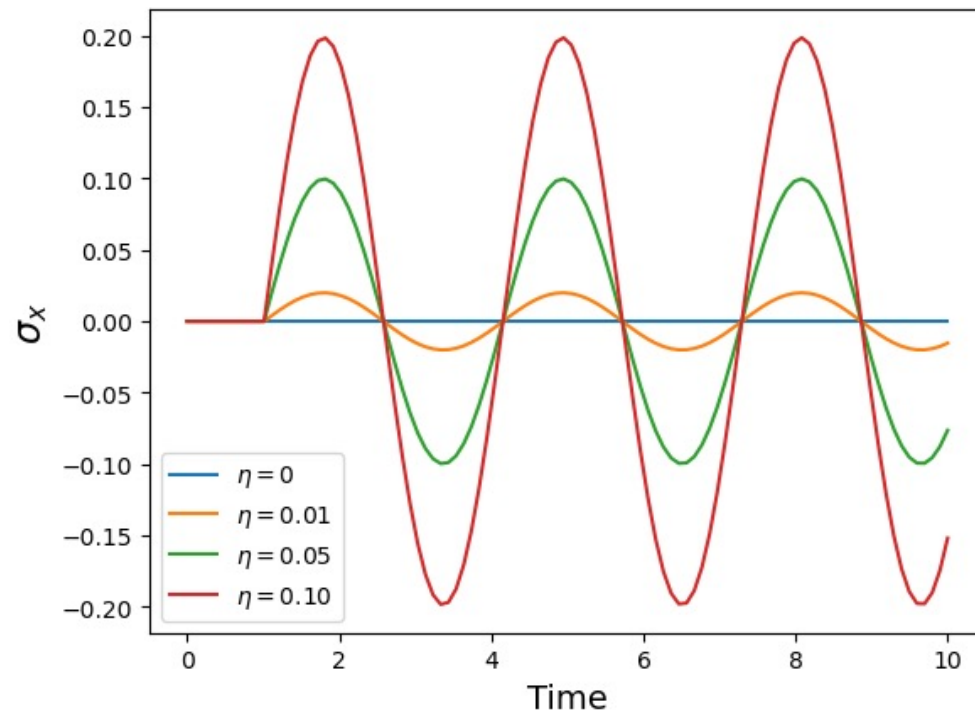
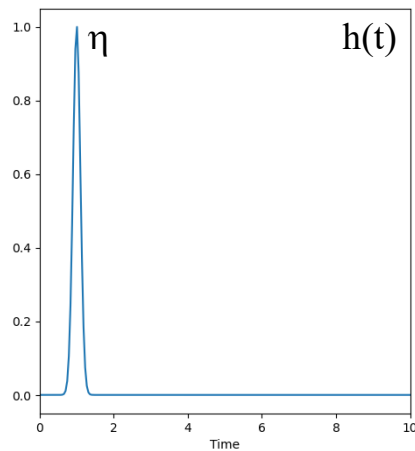


Linear Response

A simple example: single spin with energy level difference = 2

$$\mathbf{H}_0 = \sigma^z$$

$$\mathbf{A} = \mathbf{B} = \sigma^x$$

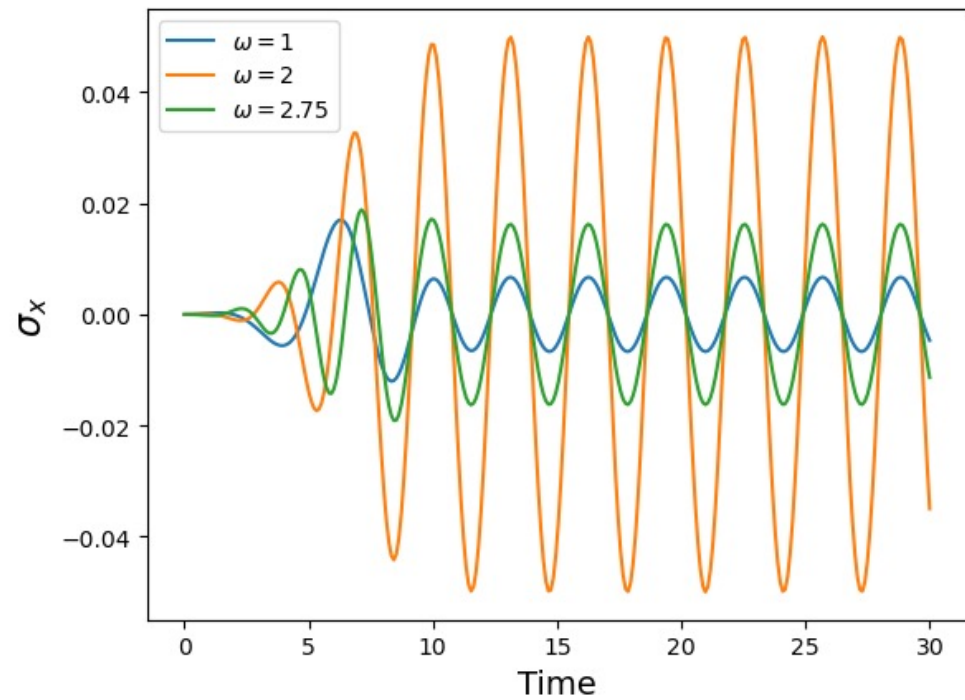
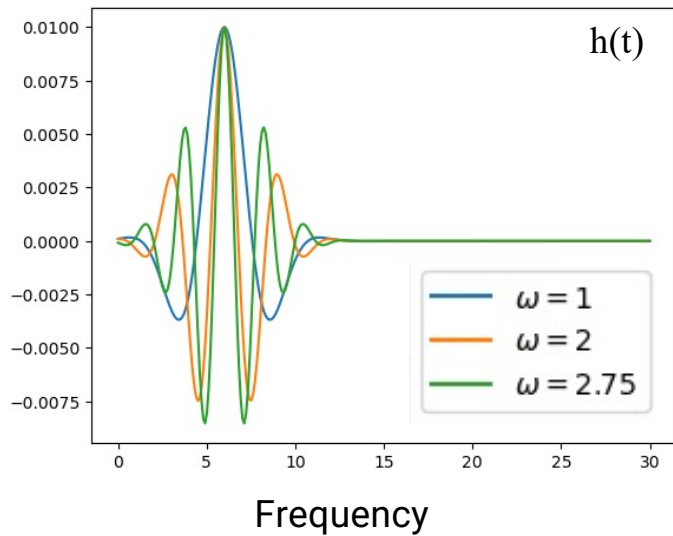


Linear Response

A simple example: single spin with energy level difference = 2

$$\mathbf{H}_0 = \sigma^z$$

$$\mathbf{A} = \mathbf{B} = \sigma^x$$

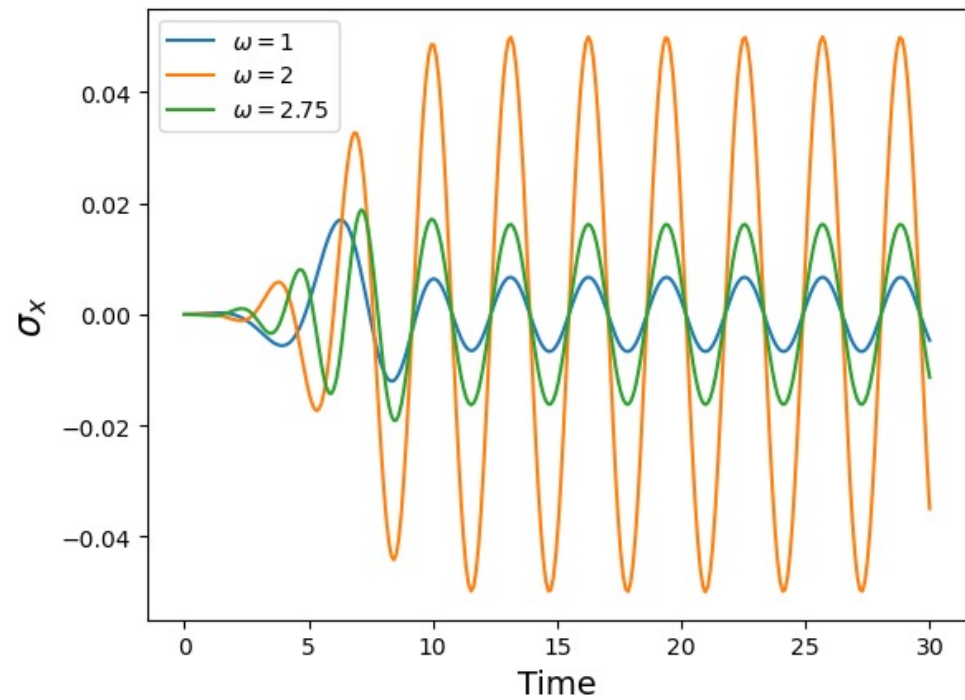
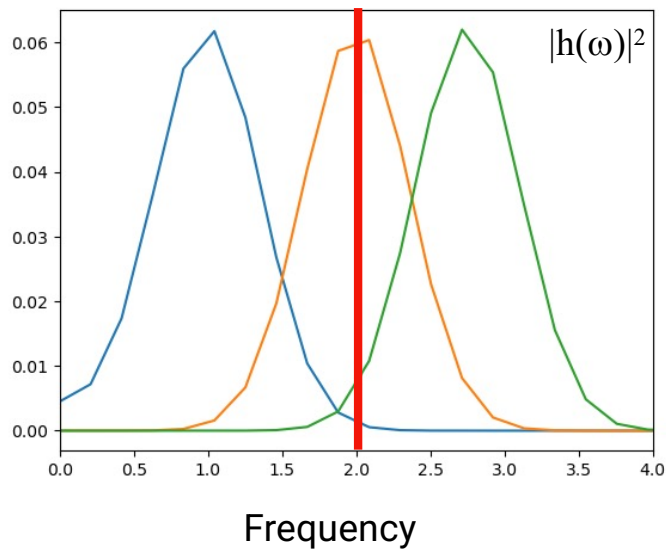


Linear Response

A simple example: single spin with energy level difference = 2

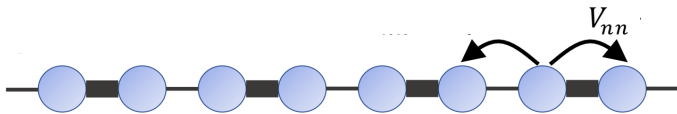
$$\mathbf{H}_0 = \sigma^z$$

$$\mathbf{A} = \mathbf{B} = \sigma^x$$

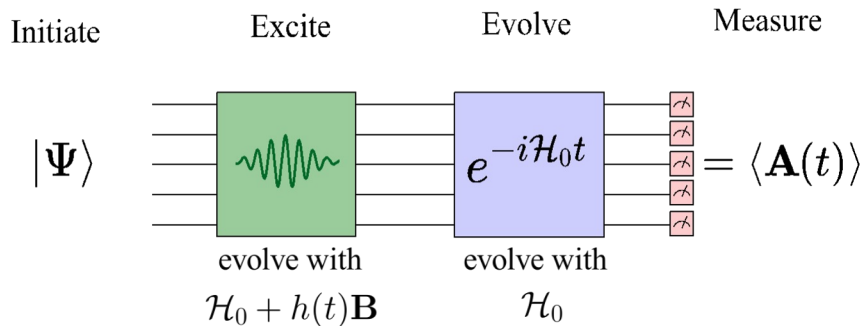


A Bosonic Correlation function: Polarizability

1D fermion chain



$$\mathcal{H}_0 = - \sum_i V_{nn} c_i^\dagger c_{i+1} + \text{h.c.}$$

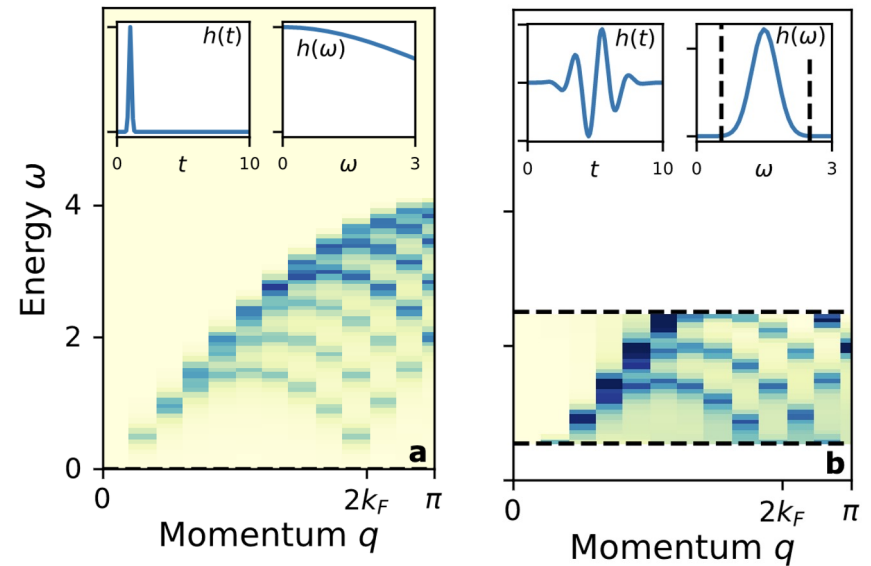


$$A(t) = A \int \omega dt' \chi^R(\mathbf{r}(t'), \mathbf{h}(t')) + \mathcal{O}(\hbar^2)$$

$$\chi(r, t) = -i \langle \psi_0 | \delta n(r, t) \delta n(r=0, t=0) | \psi_0 \rangle$$

Measure density on all sites ($\mathbf{A}=\mathbf{n}_i$)

Wiggle potential on site 0 ($\mathbf{B}=\mathbf{n}_0 V_0$)



Fermionic Linear Response

$$\left. \frac{\delta A(t)}{\delta h(t')} \right|_{h=0} = -i\theta(t-t') \langle \psi_0 | [\mathbf{A}(t), \mathbf{B}(t')] | \psi_0 \rangle$$

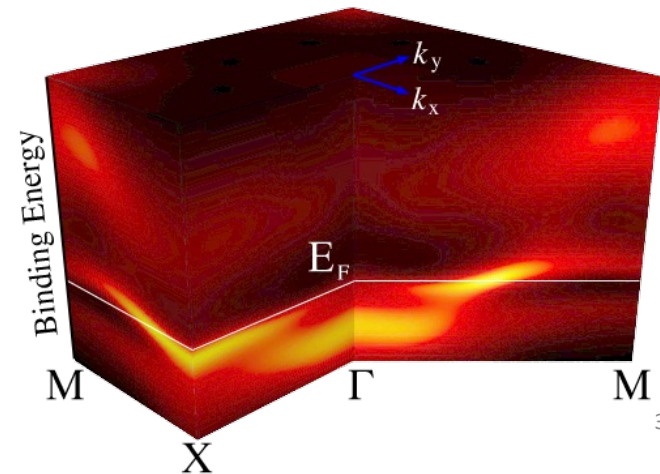
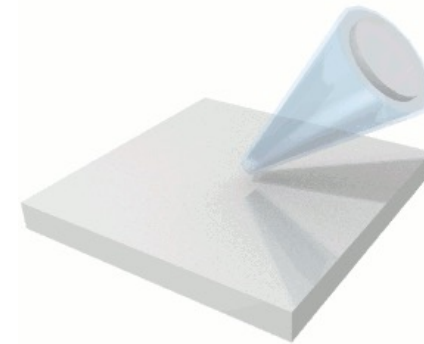
Notice this is a commutator...
... we might also want to have an anti-commutator

$$G(t, t') = -i\theta(t-t') \langle \psi_0 | \{ \mathbf{A}(t), \mathbf{B}(t') \} | \psi_0 \rangle$$

Why?

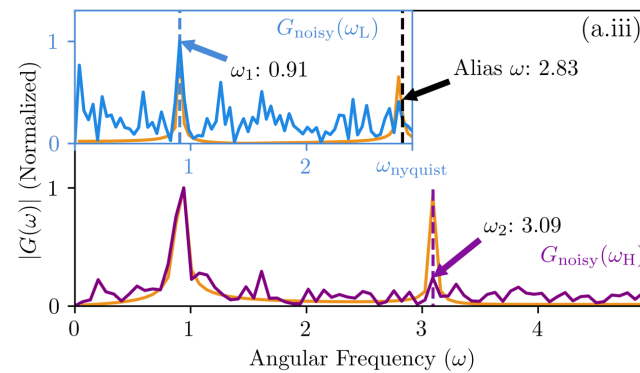
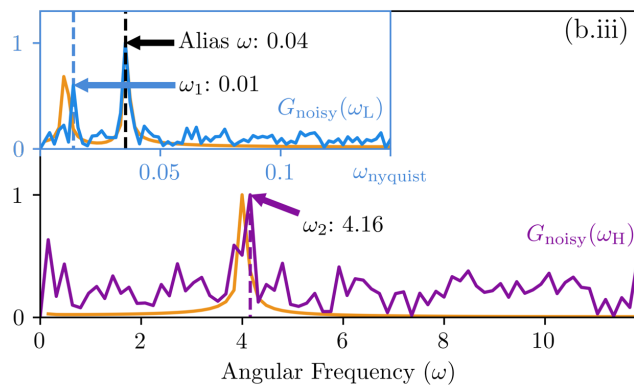
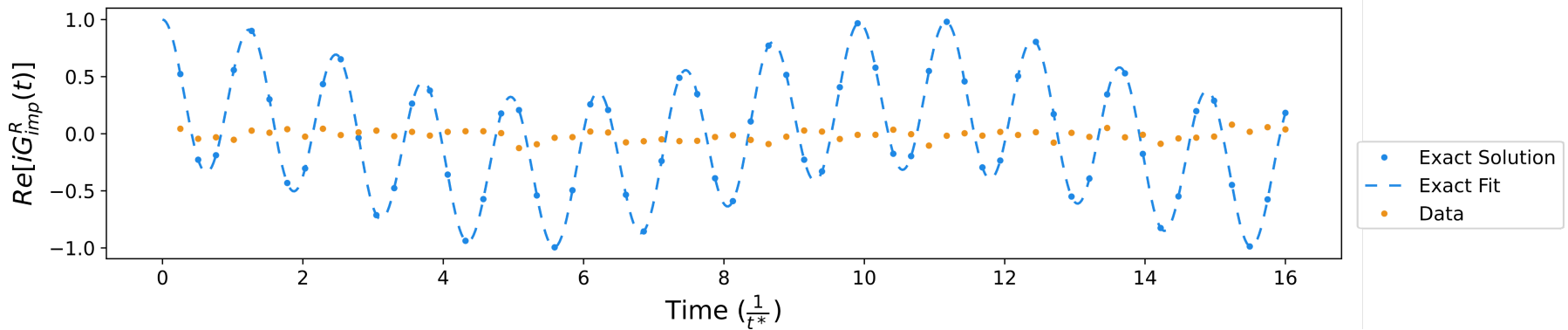
$$G^R(r_i, t; r_j, t') = -i\theta(t-t') \langle \psi_0 | \{ c_i(t), c_j^\dagger(t') \} | \psi_0 \rangle$$

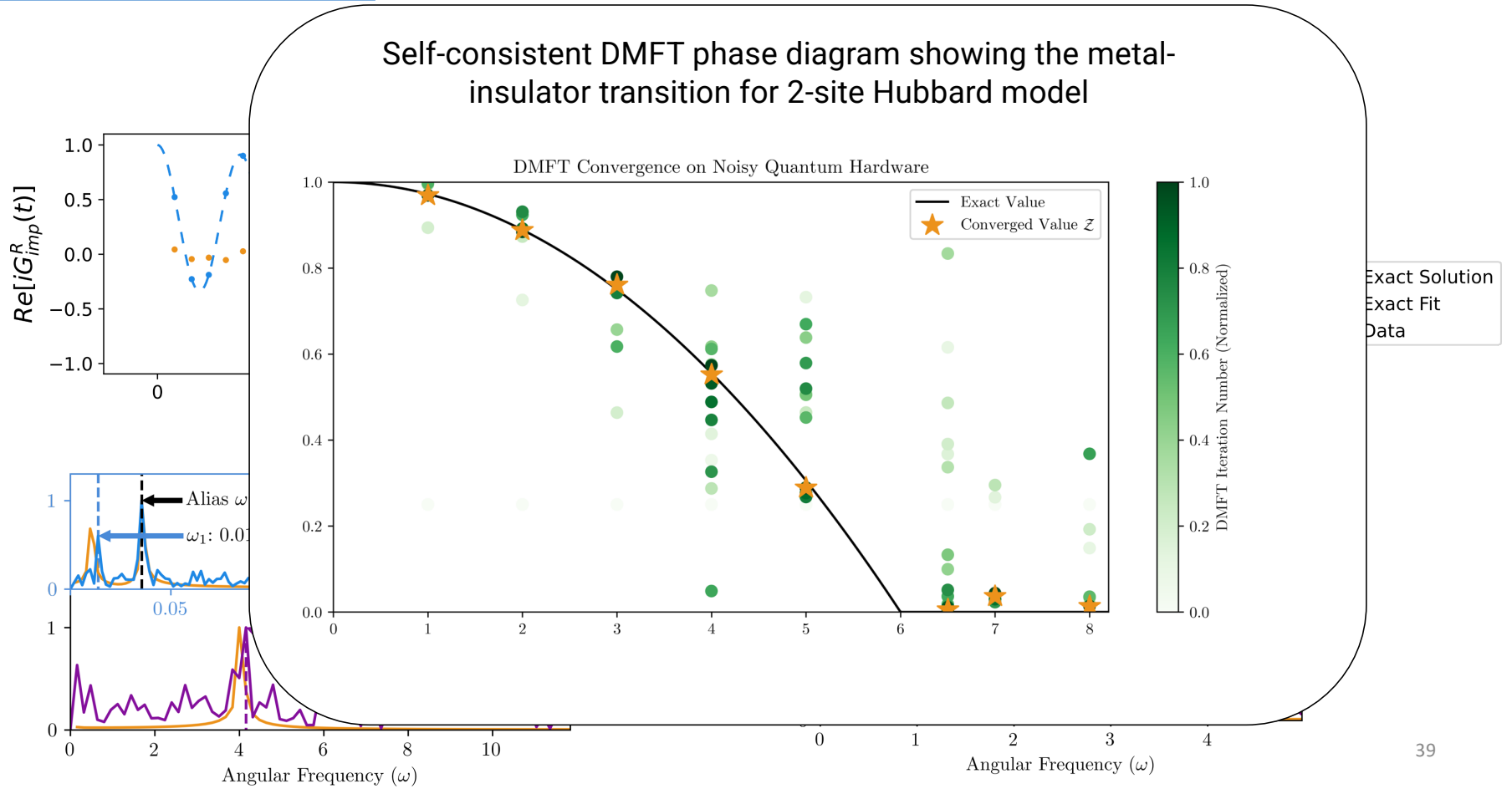
Fermionic creation/
annihilation operators



2-site Hubbard DMFT (5 qubits)

Cartan Based Simulation on IBM Lagos





Option 1: Auxiliary operator

$$\left. \frac{\delta A(t)}{\delta h(t')} \right|_{h=0} = -i\theta(t-t') \langle \psi_0 | [\mathbf{A}(t), \mathbf{B}(t')] | \psi_0 \rangle$$

Find an operator \mathbf{P} such that:

$$\{\mathbf{B}(t), \mathbf{P}\} = 0$$

$$[\mathcal{H}_0, \mathbf{P}] = 0$$

$$\mathbf{P}|\psi_0\rangle = s|\psi_0\rangle$$

Then:

$$\begin{aligned} G(t, t') &= -i\theta(t-t') \langle \psi_0 | \{\mathbf{A}(t), \mathbf{B}(t')\} | \psi_0 \rangle \\ &= \frac{i}{s} \theta(t-t') \langle \psi_0 | [\mathbf{A}(t)\mathbf{P}(t), \mathbf{B}(t')] | \psi_0 \rangle \end{aligned}$$

Example: parity

$$\mathbf{P} = Z_1 Z_2 \dots Z_n$$

Option 2: Post-selection

Option 1: Auxiliary operator

$$\left. \frac{\delta A(t)}{\delta h(t')} \right|_{h=0} = -i\theta(t-t') \langle \psi_0 | [\mathbf{A}(t), \mathbf{B}(t')] | \psi_0 \rangle$$

Find an operator \mathbf{P} such that:

$$\{\mathbf{B}(t), \mathbf{P}\} = 0$$

$$[\mathcal{H}_0, \mathbf{P}] = 0$$

$$\mathbf{P}|\psi_0\rangle = s|\psi_0\rangle$$

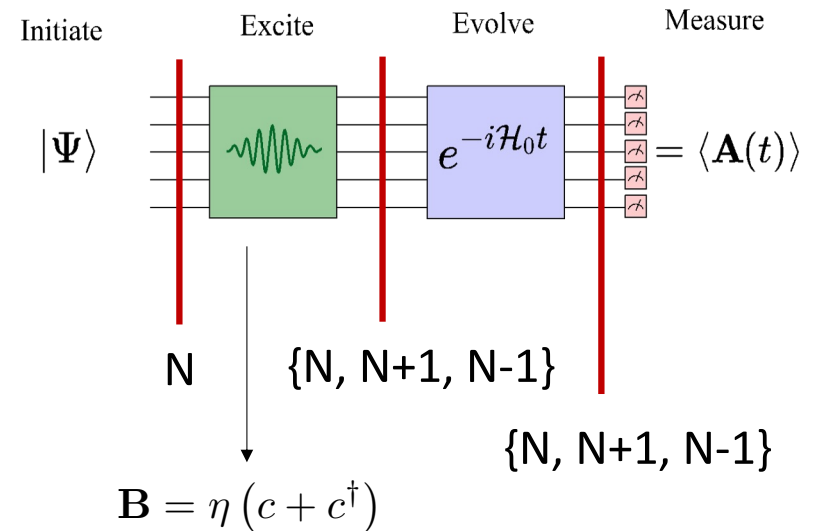
Then:

$$\begin{aligned} G(t, t') &= -i\theta(t-t') \langle \psi_0 | \{\mathbf{A}(t), \mathbf{B}(t')\} | \psi_0 \rangle \\ &= \frac{i}{s} \theta(t-t') \langle \psi_0 | [\mathbf{A}(t)\mathbf{P}(t), \mathbf{B}(t')] | \psi_0 \rangle \end{aligned}$$

Example: parity

$$\mathbf{P} = Z_1 Z_2 \dots Z_n$$

Option 2: Post-selection

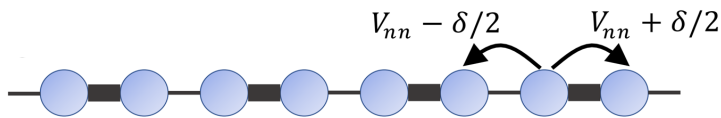


Post-selection on particle number gives us

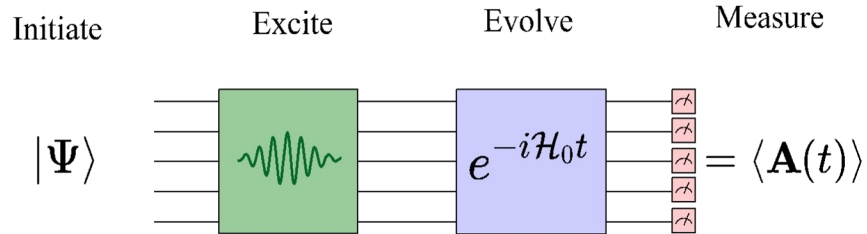
$$G_{ij}^<(t) = i \langle \psi_0 | c_j^\dagger(0) c_i(t) | \psi_0 \rangle$$

$$G_{ij}^>(t) = -i \langle \psi_0 | c_i(t) c_j^\dagger(0) | \psi_0 \rangle$$

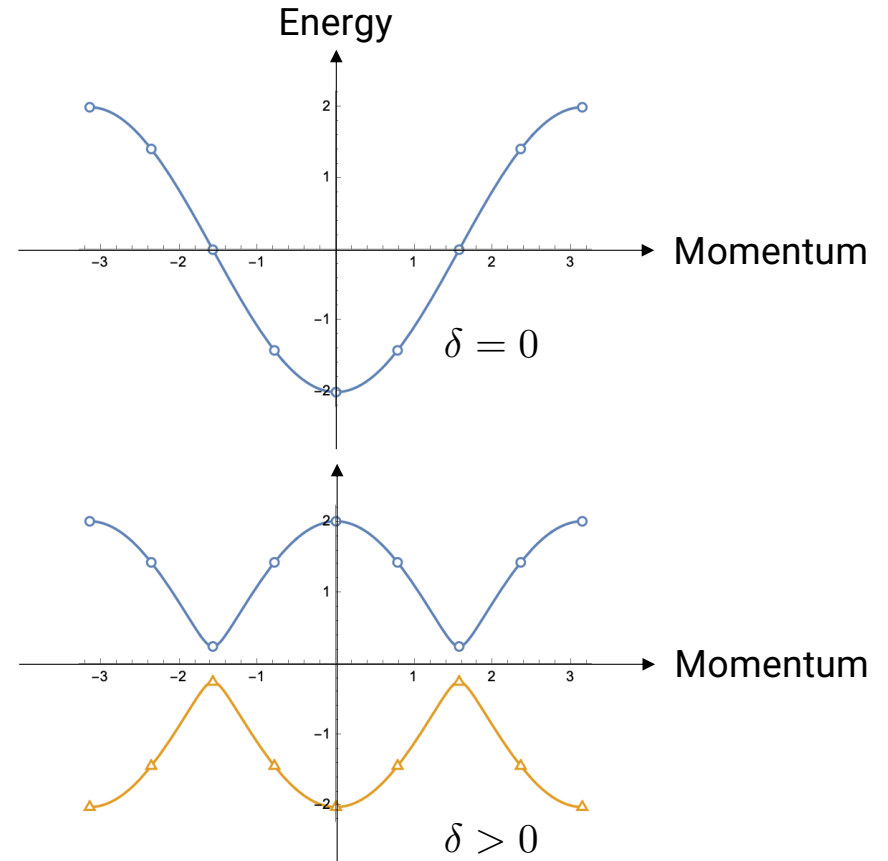
Su-Schrieffer-Heeger model for polyacetylene



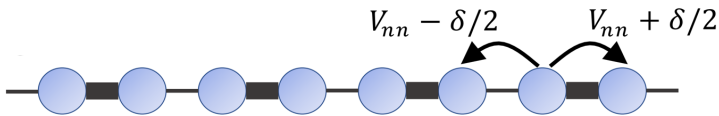
$$\mathcal{H}_0 = - \sum_{\langle i,j \rangle} \left[V_{nn} + (-1)^i \delta/2 \right] c_i^\dagger c_j - \mu \sum_i c_i^\dagger c_i$$



$$G^R(r_i, t; r_j, t') = -i\theta(t - t') \langle \psi_0 | \{c_i(t), c_j^\dagger(t')\} | \psi_0 \rangle$$

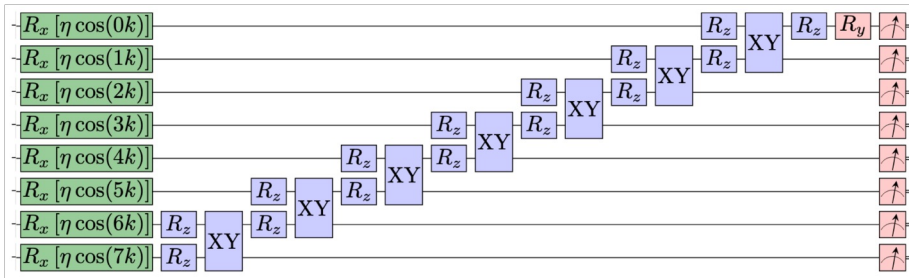


Su-Schrieffer-Heeger model for polyacetylene



$$\mathcal{H}_0 = - \sum_{\langle i,j \rangle} \left[V_{nn} + (-1)^i \delta/2 \right] c_i^\dagger c_j - \mu \sum_i c_i^\dagger c_i$$

Compressed circuit run on *ibm_auckland*

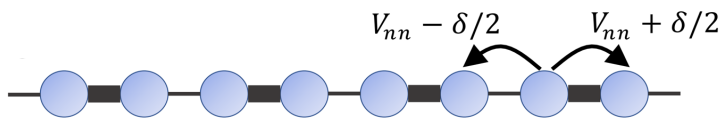


$$\mathbf{B} = \sum_i 2 \cos(kr_i) \left[c_i + c_i^\dagger \right]$$

Choose \mathbf{B} to create a momentum eigenstate

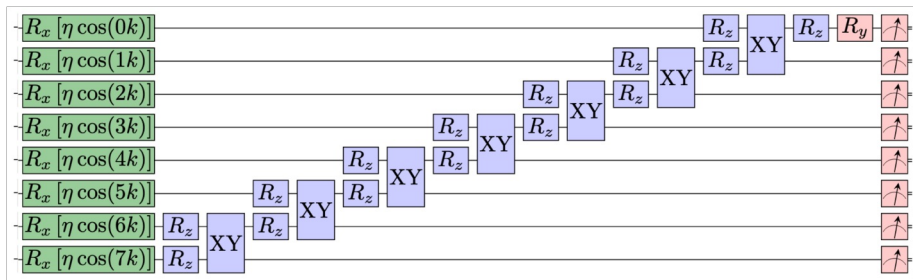
$$G_k^R(t) = -i\theta(t) \langle \psi_0 | \{ c_k(t), c_k^\dagger(0) \} | \psi_0 \rangle$$

Su-Schrieffer-Heeger model for polyacetylene



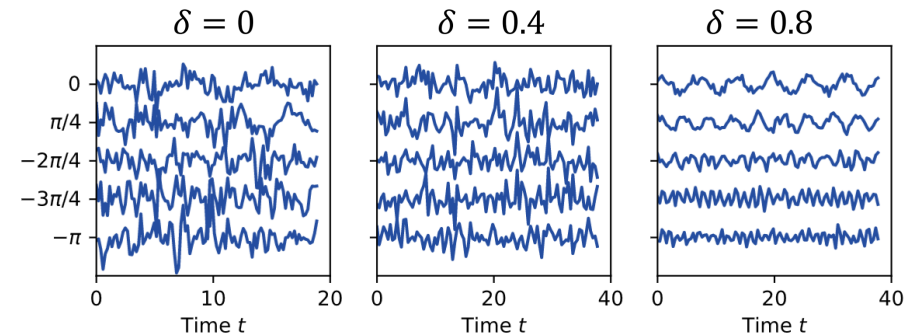
$$\mathcal{H}_0 = - \sum_{\langle i,j \rangle} \left[V_{nn} + (-1)^i \delta/2 \right] c_i^\dagger c_j - \mu \sum_i c_i^\dagger c_i$$

Compressed circuit run on *ibm_auckland*

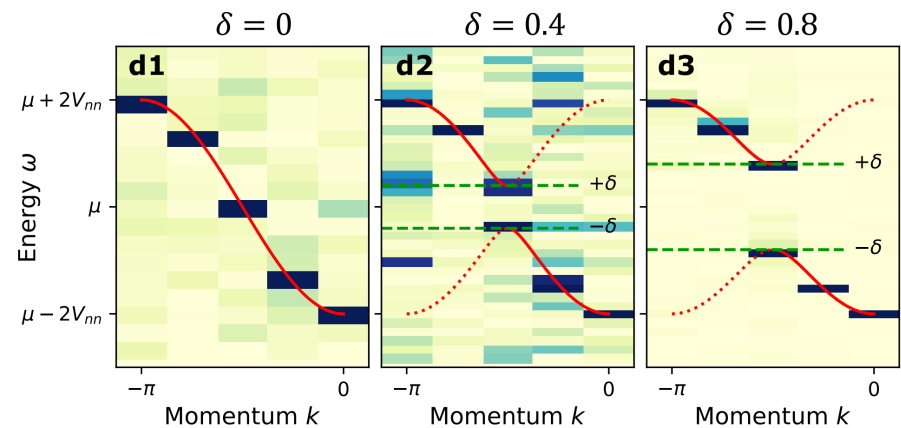


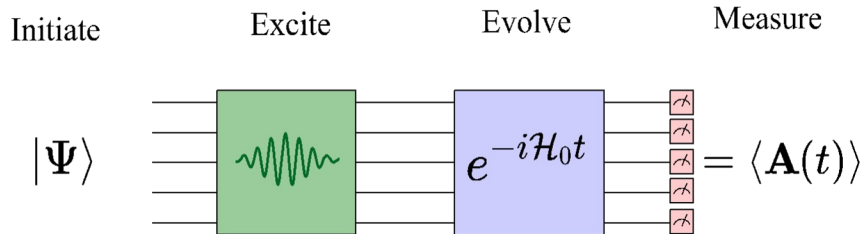
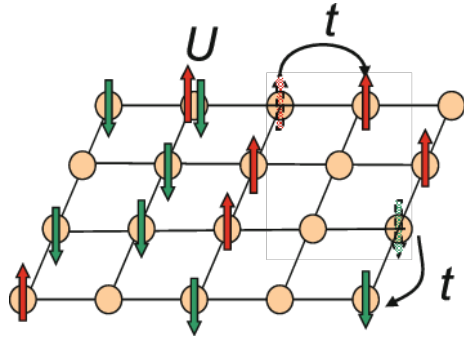
Choose **B** to create a momentum eigenstate

$$G_k^R(t) = -i\theta(t) \langle \psi_0 | \{c_k(t), c_k^\dagger(0)\} | \psi_0 \rangle$$



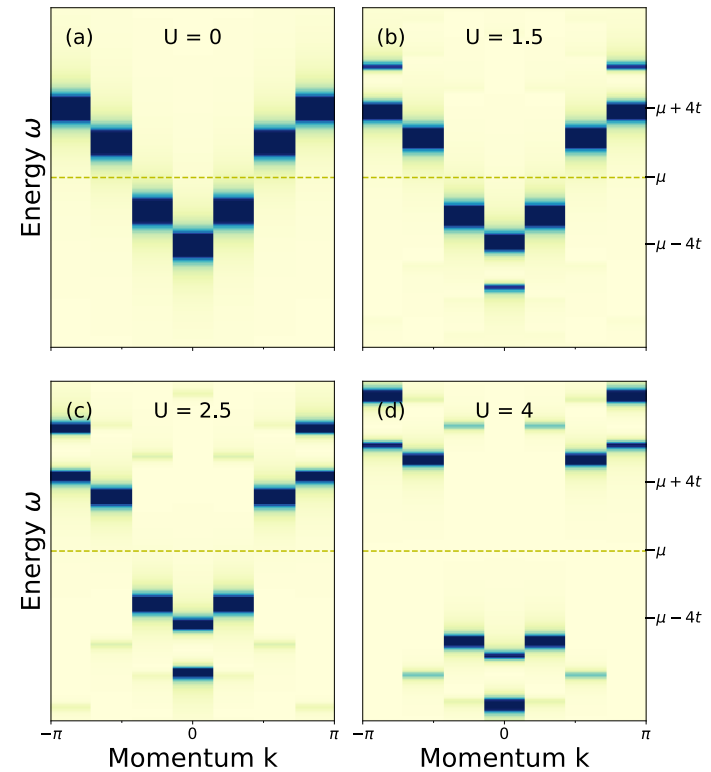
Fourier

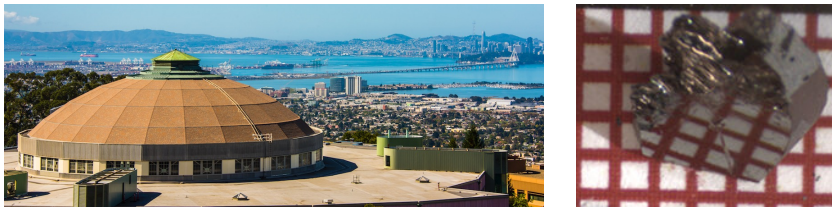




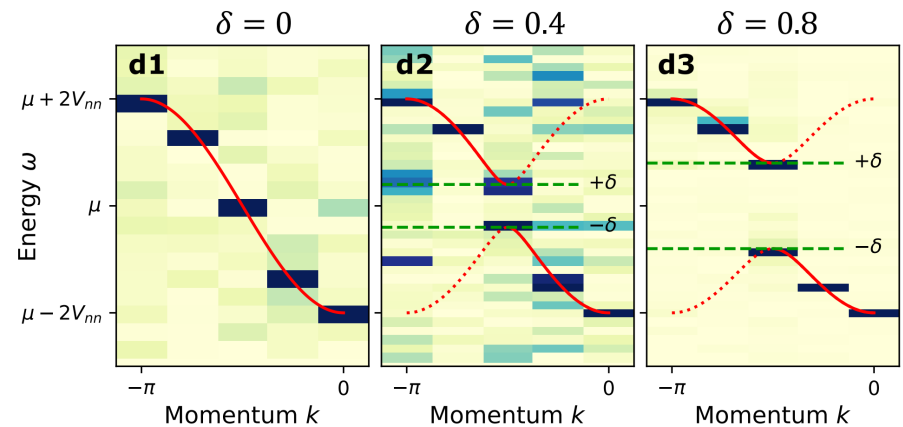
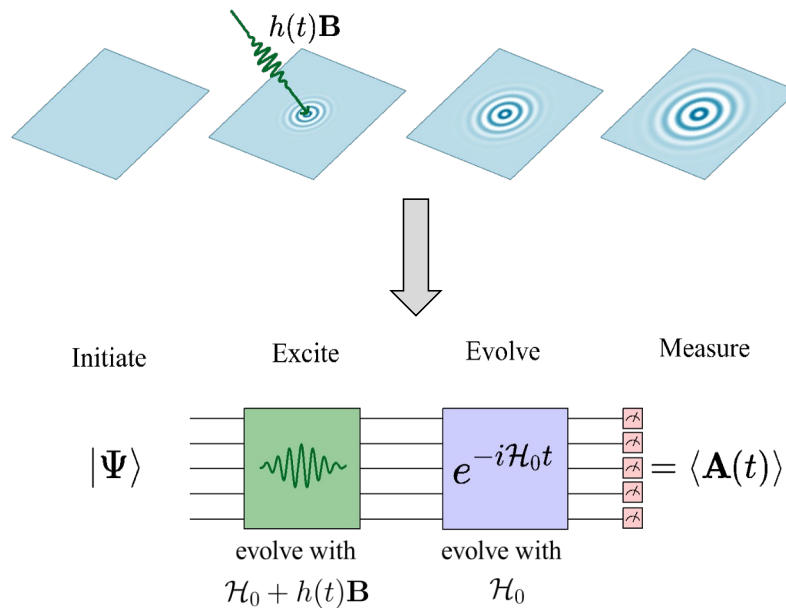
Choose \mathbf{B} to create a momentum eigenstate

$$G_k^R(t) = -i\theta(t)\langle \psi_0 | \{c_k(t), c_k^\dagger(0)\} | \psi_0 \rangle$$





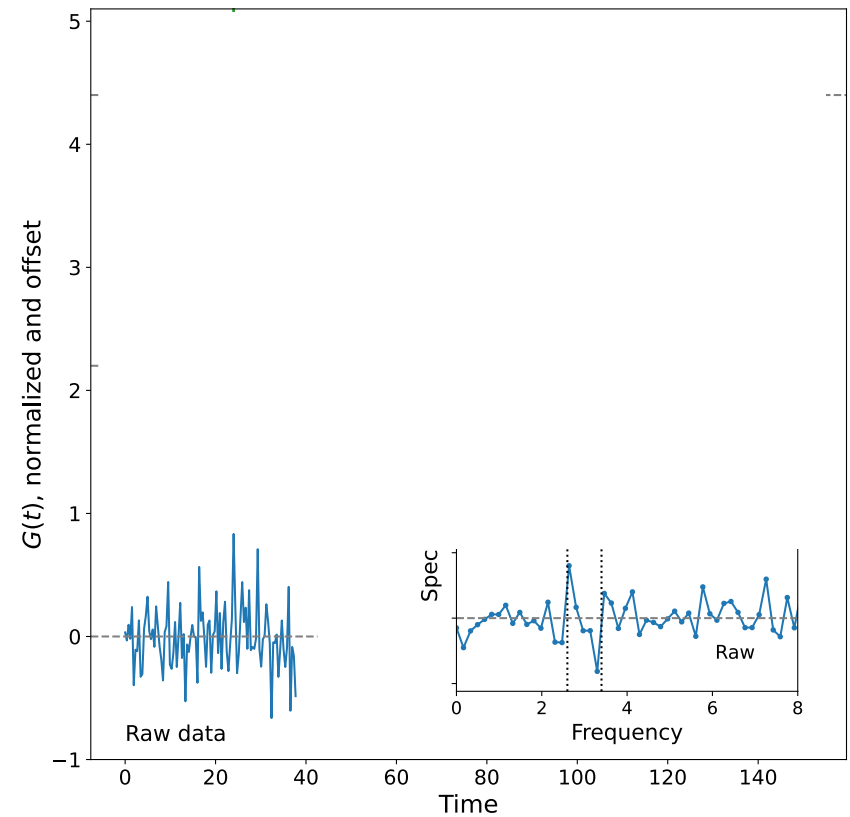
- Ancilla free
- Momentum and frequency selectivity
- Both bosonic and fermionic correlators
- More noise robust compared to existing methods



Further improvements via mathematics

- It turns out that these are positive semi-definite functions:

$$\langle A^\dagger(t) A(t') \rangle$$

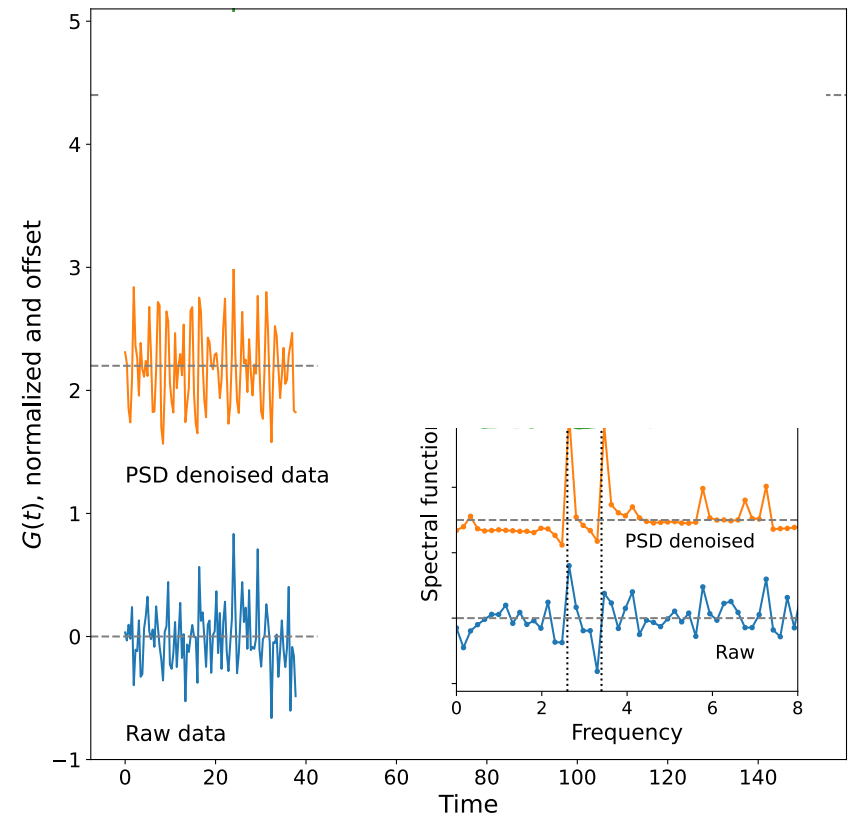


Further improvements via mathematics

- It turns out that these are positive semi-definite functions:

$$\langle A^\dagger(t)A(t') \rangle$$

- We can project the noisy data onto the nearest PSD function

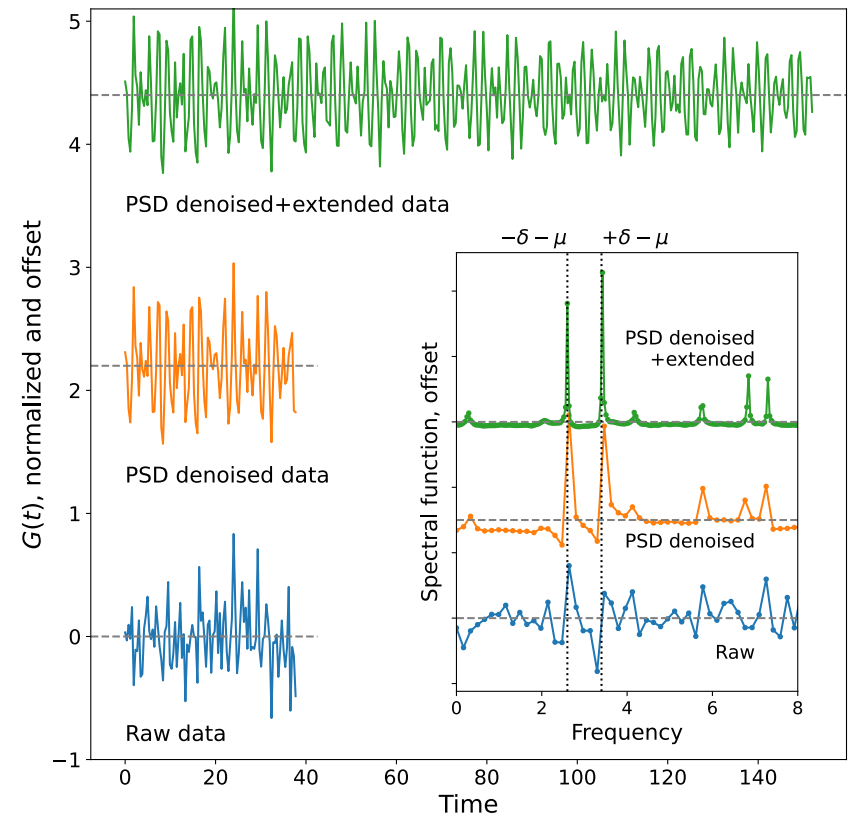


Further improvements via mathematics

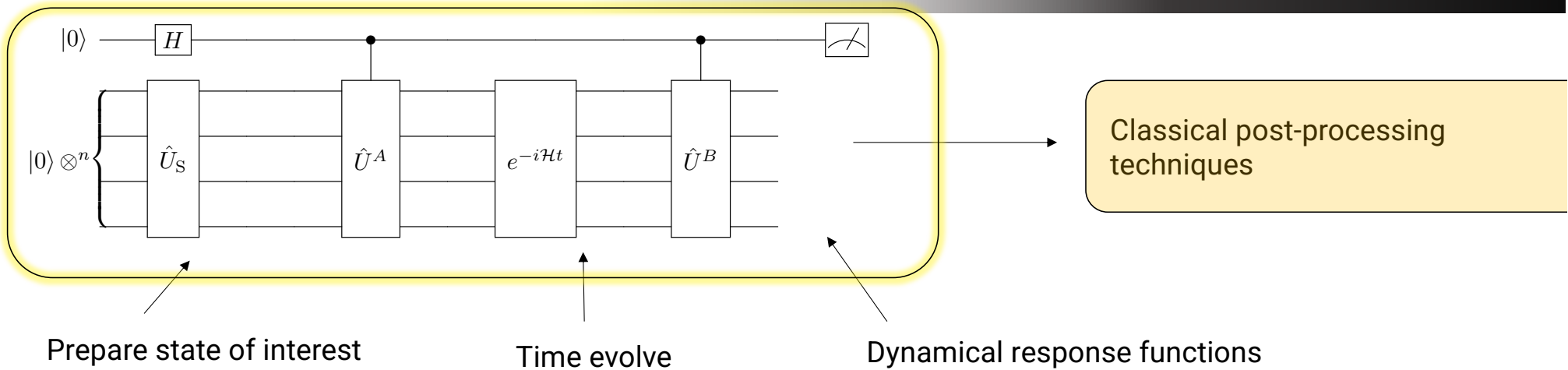
- It turns out that these are positive semi-definite functions:

$$\langle A^\dagger(t)A(t') \rangle$$

- We can project the noisy data onto the nearest PSD function
- Given sufficiently dense data, a unique extension exists* and we can extend the data to longer times



A-Z quantum simulation



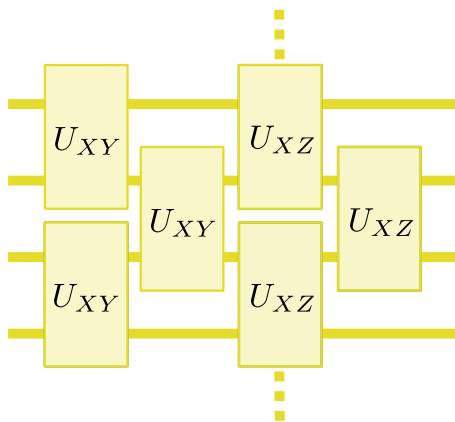
- *Physics-Informed Subspace Expansions*

- *Lie-algebraic methods for time evolution*
- *Open quantum system evolution*

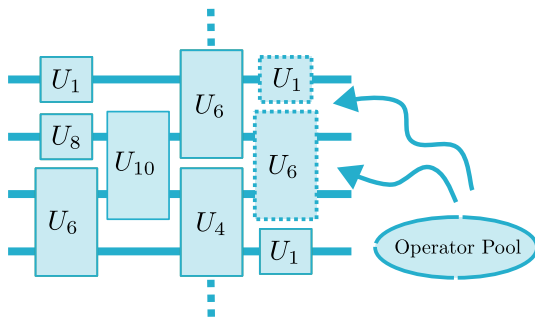
- *Neutron scattering (magnon) spectra*
- *Open quantum system Green's functions*
- *Dynamical Mean Field Theory*

Lie algebraic methods for quantum computing

Time evolution



Variational ansätze

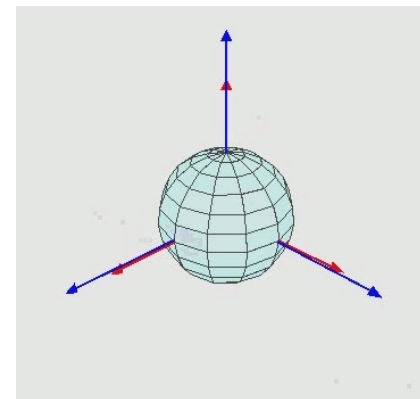


Dynamical Lie algebras

Given a set of operators a_i (either in the operator pool or Hamiltonian)

Their Dynamical Lie Algebra expresses all the operators that can be generated by this set

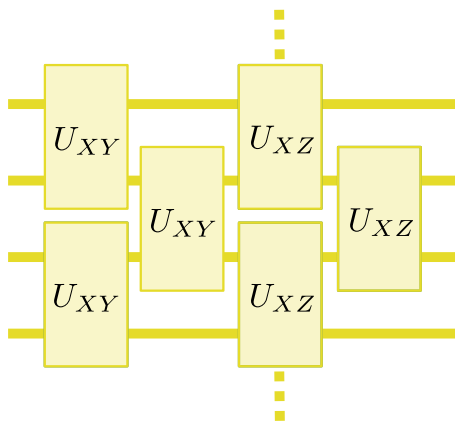
$$DLA := \text{span}\{[a_{i_1}, [a_{i_2}, [\dots [a_{i_r}, a_j] \dots]]]\}$$



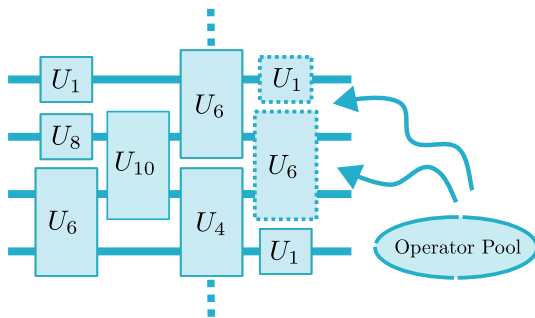
By Euler2.gif: Juansemperederivative work: Xavax - This file was derived from: Euler2.gif, CC BY-SA 3.0, <https://commons.wikimedia.org/w/index.php?curid=24338647>

Lie algebraic methods for quantum computing

Time evolution



Variational ansätze



Dynamical Lie algebras

Given a set of operators a_i (either in the operator pool or Hamiltonian)

Their Dynamical Lie Algebra expresses all the operators that can be generated by this set

$$DLA := \text{span}\{[a_{i_1}, [a_{i_2}, [\dots [a_{i_r}, a_j] \dots]]]\}$$

Cartan decomposition for exact time evolution

Kökcü, PRL 2022

Circuit compression

Kökcü, PRA 2022

Camps, SIMAX 2022

Kökcü, arXiv:2303.09538

Unified Framework for Barren plateaus in VQA

Ragone, arXiv:2309.09342

Complete (DLA) classification of 1-d nearest neighbor spin models

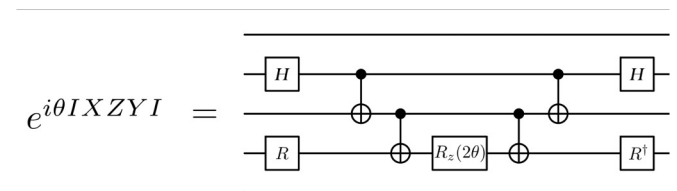
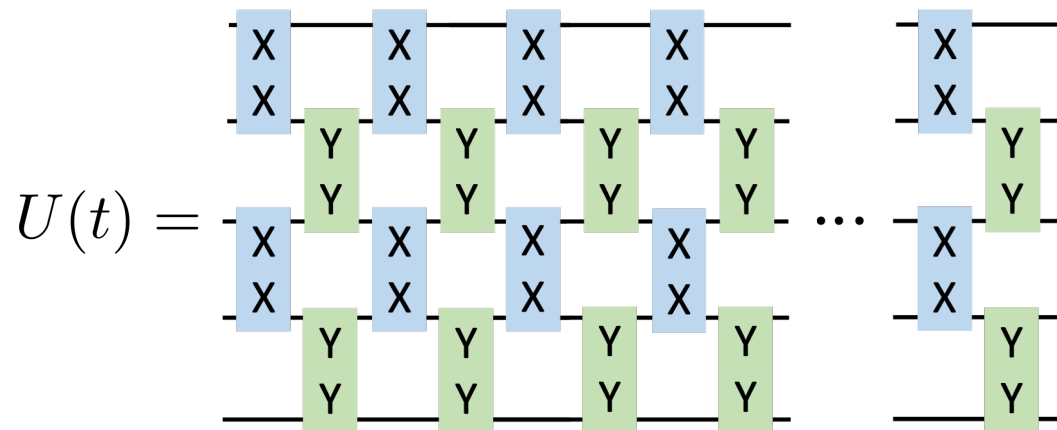
Wiersema, arXiv:2309.05690

Main Problem

Exact simulation of a time independent spin Hamiltonian: $\mathcal{H} = \sum_j h_j \sigma^j$

$$\mathcal{H} = a XXIII + b IYYII + c IIXXI + d IIIYY$$

$$U(\epsilon) = e^{-i\epsilon\mathcal{H}} = e^{-i\epsilon a XXIII} e^{-i\epsilon b IYYII} e^{-i\epsilon c IIXXI} e^{-i\epsilon d IIIYY} + O(\epsilon^2)$$

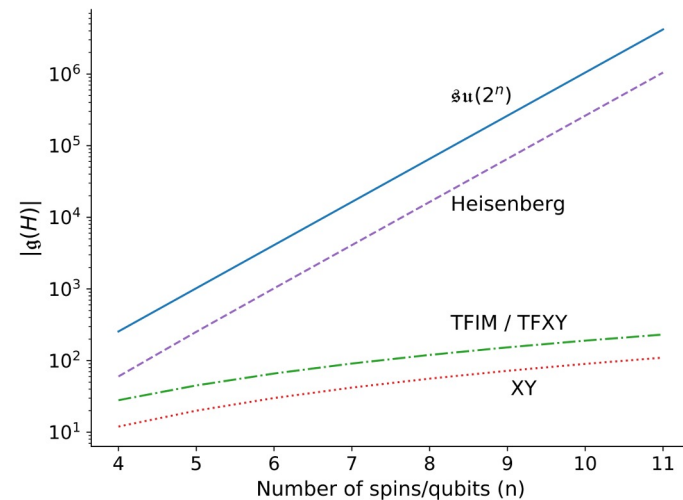
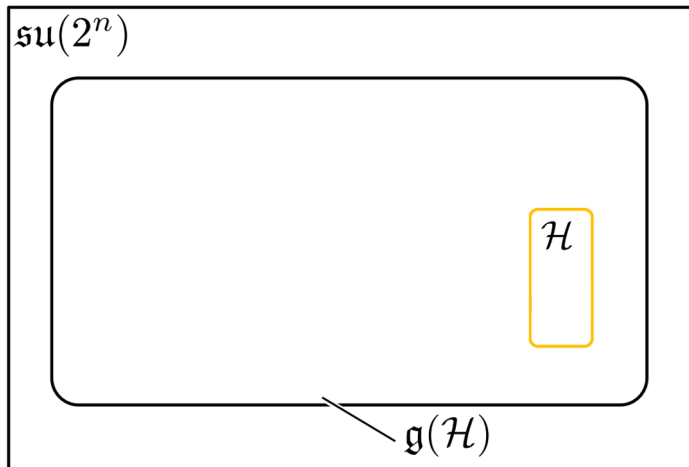


Main Problem

Exact simulation of a time independent spin Hamiltonian: $\mathcal{H} = \sum_j h_j \sigma^j$

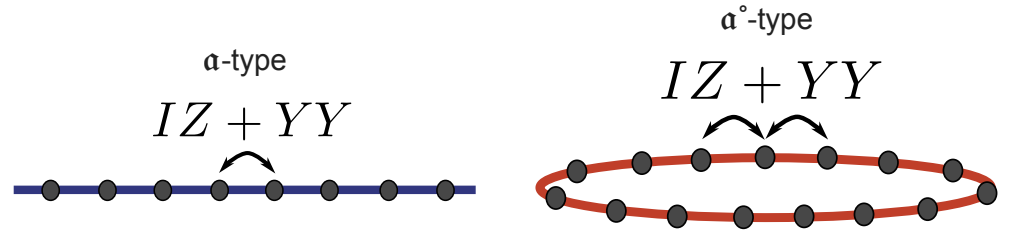
$$U(t) = e^{-it\mathcal{H}} = \prod_{\substack{\bar{\sigma}^i \in \mathfrak{su}(2^n) \\ \bar{\sigma}^i \in \mathfrak{g}(\mathcal{H})}} e^{i\kappa_i \bar{\sigma}^i}$$

$$\text{DLA} := \text{span}\{[a_{i_1}, [a_{i_2}, [\dots [a_{i_r}, a_j] \dots]]]\}$$

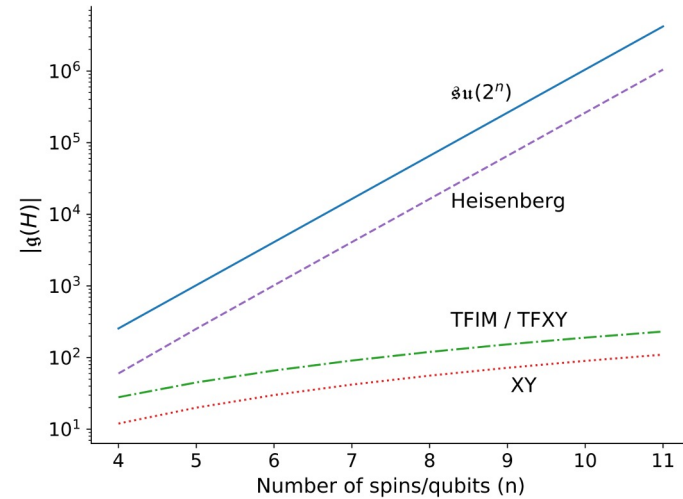


$\mathfrak{a}_0(n)$	$= \text{span}\{X_j, X_{j+1}\}_{1 \leq j \leq n-1} \cong \mathfrak{u}(1)^{\oplus(n-1)}$	$\dim = n - 1,$	
$\mathfrak{a}_1(n)$	$= \text{span}\{X_i, Z_{i+1} \cdots Z_{j-1} Y_j\}_{1 \leq i < j \leq n} \cong \mathfrak{so}(n),$	$\dim = \frac{n(n-1)}{2},$	
$\mathfrak{a}_2(n)$	$= \text{span}\{X_i, Z_{i+1} \cdots Z_{j-1} Y_j\}_{1 \leq i < j \leq n} \oplus \text{span}\{Y_i, Z_{i+1} \cdots Z_{j-1} X_j\}_{1 \leq i < j \leq n}$	$\cong \mathfrak{so}(n) \oplus \mathfrak{so}(n), \dim = n(n-1),$	
$\mathfrak{a}_3(n)$	$\cong \begin{cases} \mathfrak{so}(2^{n-2})^{\oplus 4}, & \dim = 2^{n-1}(2^{n-2} - 1), & n \equiv 0 \pmod{8}, \\ \mathfrak{so}(2^{n-1}), & \dim = 2^{n-2}(2^{n-1} - 1), & n \equiv \pm 1 \pmod{8}, \\ \mathfrak{su}(2^{n-2})^{\oplus 2}, & \dim = 2^{2n-3} - 2, & n \equiv \pm 2 \pmod{8}, \\ \mathfrak{sp}(2^{n-2}), & \dim = 2^{n-2}(2^{n-1} + 1), & n \equiv \pm 3 \pmod{8}, \\ \mathfrak{sp}(2^{n-3})^{\oplus 4}, & \dim = 2^{n-1}(2^{n-2} + 1), & n \equiv 4 \pmod{8}, \end{cases}$		
	$\mathfrak{a}_4(n) \cong \mathfrak{a}_2(n),$		
	$\mathfrak{a}_5(n)$	$\cong \begin{cases} \mathfrak{so}(2^{n-2})^{\oplus 4}, & \dim = 2^{n-1}(2^{n-2} - 1), & n \equiv 0 \pmod{6}, \\ \mathfrak{so}(2^{n-1}), & \dim = 2^{n-2}(2^{n-1} - 1), & n \equiv \pm 1 \pmod{6}, \\ \mathfrak{su}(2^{n-2})^{\oplus 2}, & \dim = 2^{2n-3} - 2, & n \equiv \pm 2 \pmod{6}, \\ \mathfrak{sp}(2^{n-2}), & \dim = 2^{n-2}(2^{n-1} + 1), & n \equiv 3 \pmod{6}, \end{cases}$	
		$\mathfrak{a}_6(n) \cong \mathfrak{a}_7(n) \cong \mathfrak{a}_{10}(n) \cong \begin{cases} \mathfrak{su}(2^{n-1}), & \dim = 2^{2n-2} - 1, & n \text{ odd}, \\ \mathfrak{su}(2^{n-2})^{\oplus 4}, & \dim = 2^{2n-2} - 4, & n \geq 4 \text{ even}, \end{cases}$	
$\mathfrak{a}_8(n)$	$\cong \mathfrak{so}(2n - 1), \dim = (n - 1)(2n - 1),$		
$\mathfrak{a}_9(n)$	$\cong \mathfrak{sp}(2^{n-2}), \dim = 2^{n-2}(2^{n-1} + 1),$		
$\mathfrak{a}_{11}(n)$	$= \mathfrak{a}_{16}(n) = \mathfrak{so}(2^n), \dim = 2^{n-1}(2^n - 1), \quad n \geq 4,$		
$\mathfrak{a}_k(n)$	$= \mathfrak{su}(2^n), \dim = 2^{2n} - 1, \quad k = 12, 17, 18, 19, 21, 22, \quad n \geq 4,$		
$\mathfrak{a}_{13}(n)$	$= \mathfrak{a}_{20}(n) \cong \mathfrak{a}_{15}(n) \cong \mathfrak{su}(2^{n-1}) \oplus \mathfrak{su}(2^{n-1}), \dim = 2^{2n-1} - 2,$		
$\mathfrak{a}_{14}(n)$	$\cong \mathfrak{so}(2n), \dim = n(2n - 1),$		
$\mathfrak{b}_0(n)$	$= \text{span}\{X_i\}_{1 \leq i \leq n} \cong \mathfrak{u}(1)^{\oplus n}, \dim = n,$		
$\mathfrak{b}_1(n)$	$= \text{span}\{X_i, X_j, X_{j+1}\}_{1 \leq i \leq n, 1 \leq j \leq n-1} \cong \mathfrak{u}(1)^{\oplus(2n-1)}, \dim = 2n - 1,$		
$\mathfrak{b}_2(n)$	$= \mathfrak{a}_9(n) \oplus \text{span}\{X_1\} \cong \mathfrak{sp}(2^{n-2}) \oplus \mathfrak{u}(1), \dim = 2^{n-2}(2^{n-1} + 1) + 1,$		
$\mathfrak{b}_3(n)$	$= \text{span}\{X_i, Y_i, Z_i\}_{1 \leq i \leq n} \cong \mathfrak{su}(2)^{\oplus n}, \dim = 3n,$		
$\mathfrak{b}_4(n)$	$= \mathfrak{a}_{15}(n) \oplus \text{span}\{X_1\} \cong \mathfrak{su}(2^{n-1}) \oplus \mathfrak{su}(2^{n-1}) \oplus \mathfrak{u}(1), \dim = 2^{2n-1} - 1.$		

List of unique dynamical Lie algebras



$$\text{DLA} := \text{span}\{[a_{i_1}, [a_{i_2}, [\dots [a_{i_r}, a_j] \dots]]]\}$$

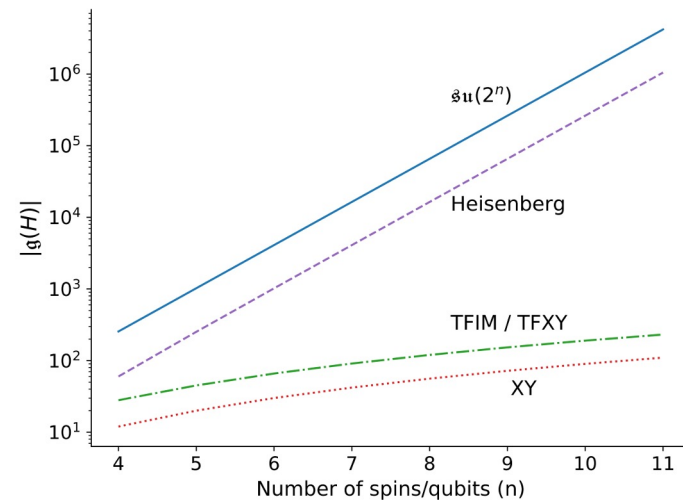
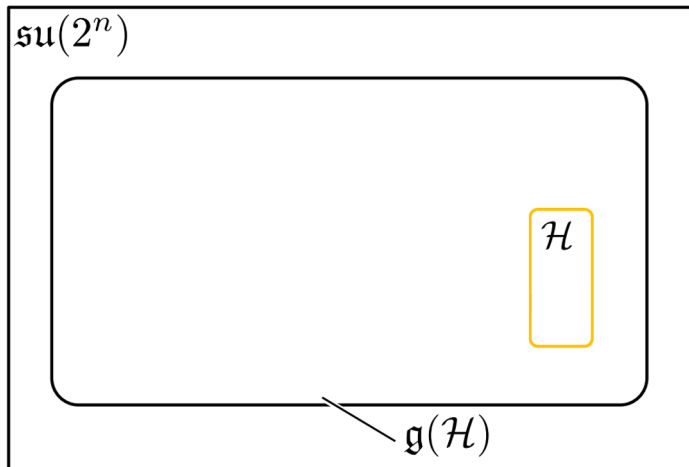


Main Problem

Exact simulation of a time independent spin Hamiltonian: $\mathcal{H} = \sum_j h_j \sigma^j$

$$U(t) = e^{-it\mathcal{H}} = \prod_{\substack{\bar{\sigma}^i \in \mathfrak{su}(2^n) \\ \bar{\sigma}^i \in \mathfrak{g}(\mathcal{H})}} e^{i\kappa_i \bar{\sigma}^i}$$

$$\text{DLA} := \text{span}\{[a_{i_1}, [a_{i_2}, [\dots [a_{i_r}, a_j] \dots]]]\}$$

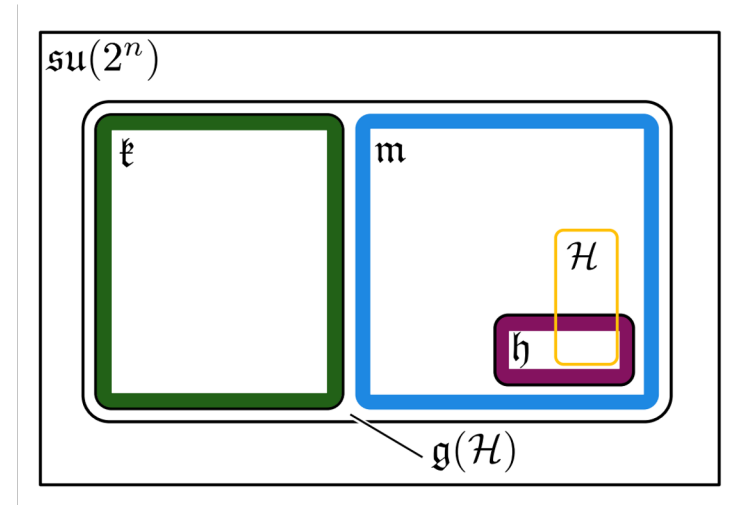


Cartan Decomposition and KHK Theorem

Definition 1 Consider a compact semi-simple Lie subgroup $G \subset SU(2^n)$, which has a corresponding Lie subalgebra \mathfrak{g} . A **Cartan decomposition** on \mathfrak{g} is defined as an orthogonal split $\mathfrak{g} = \mathfrak{k} \oplus \mathfrak{m}$ satisfying

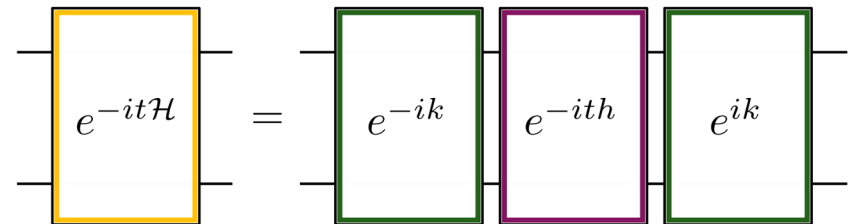
$$[\mathfrak{k}, \mathfrak{k}] \subset \mathfrak{k} \quad [\mathfrak{m}, \mathfrak{m}] \subset \mathfrak{k} \quad [\mathfrak{k}, \mathfrak{m}] = \mathfrak{m} \quad (4)$$

and is referred as $(\mathfrak{g}, \mathfrak{k})$. **Cartan subalgebra** of this decomposition is defined as one of the maximal Abelian subalgebras of \mathfrak{m} , and denoted as \mathfrak{h} .



Theorem 1 Given a Cartan decomposition $\mathfrak{g} = \mathfrak{k} \oplus \mathfrak{m}$, for any element $\mathcal{H} \in \mathfrak{m}$ there exist a $K \in e^{\mathfrak{k}}$ and $h \in \mathfrak{h}$ such that

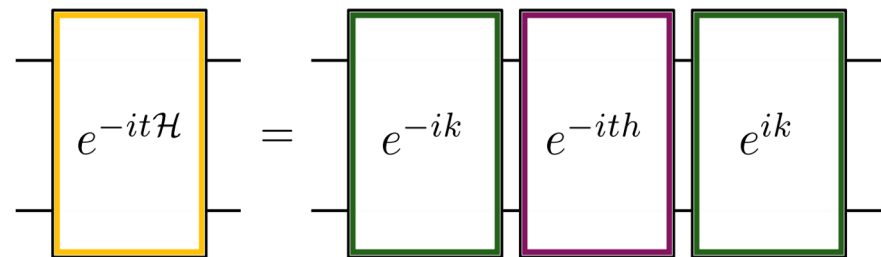
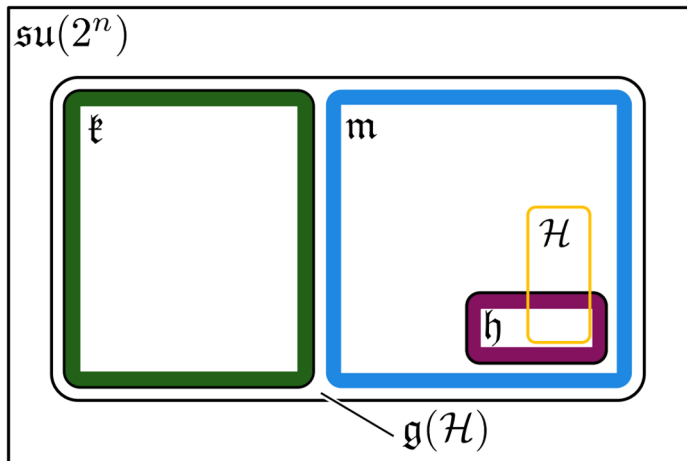
$$\mathcal{H} = KhK^\dagger \quad (5)$$



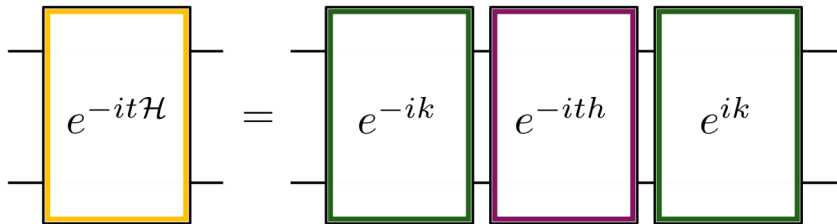
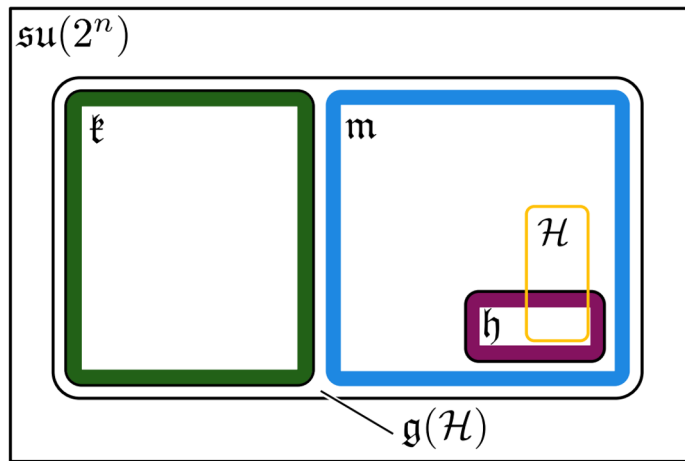
Main Problem

Exact simulation of a time independent spin Hamiltonian: $\mathcal{H} = \sum_j h_j \sigma^j$

$$U(t) = e^{-it\mathcal{H}} = \prod_{\substack{\bar{\sigma}^i \in \mathfrak{su}(2^n) \\ \bar{\sigma}^i \in \mathfrak{g}(\mathcal{H})}} e^{i\kappa_i \bar{\sigma}^i}$$



Cartan Decomposition and KHK Theorem



$$U(t) = e^{-it\mathcal{H}} = \prod_{\substack{\bar{\sigma}^i \in \mathfrak{su}(2^n) \\ \bar{\sigma}^i \in \mathfrak{g}(\mathcal{H})}} e^{i\kappa_i \bar{\sigma}^i}$$

Have $H \in \mathfrak{m}$, and consider the following function

$$f(K) = \langle K v K^\dagger H \rangle$$

where

$$K = e^{\theta_1 k_1} e^{\theta_2 k_2} \dots e^{\theta_{n_k} k_{n_k}}$$

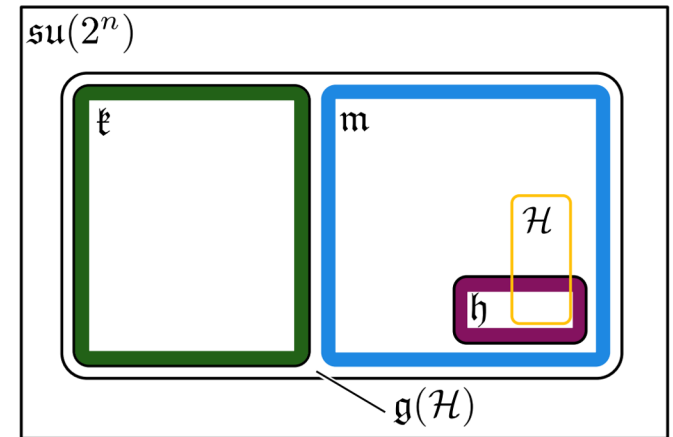
$$v = h_1 + \pi h_2 + \pi^2 h_3 + \dots + \pi^{n_h-1} h_{n_h}$$

Then for any local minimum or maximum of the function f denoted by K_0 will satisfy

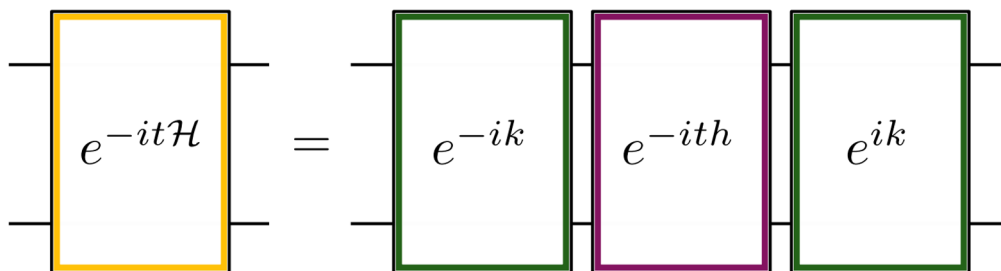
$$K_0^\dagger H K_0 \in \mathfrak{h}$$

Algorithm

- 1) Generate Hamiltonian algebra $\mathfrak{g}(H)$
- 2) Find a Cartan decomposition where H is in \mathfrak{m}
- 3) Obtain parameters via **local** minimum of $f(K)$
- 4) Build the circuit using K and h
- 5) Then simulate for any t

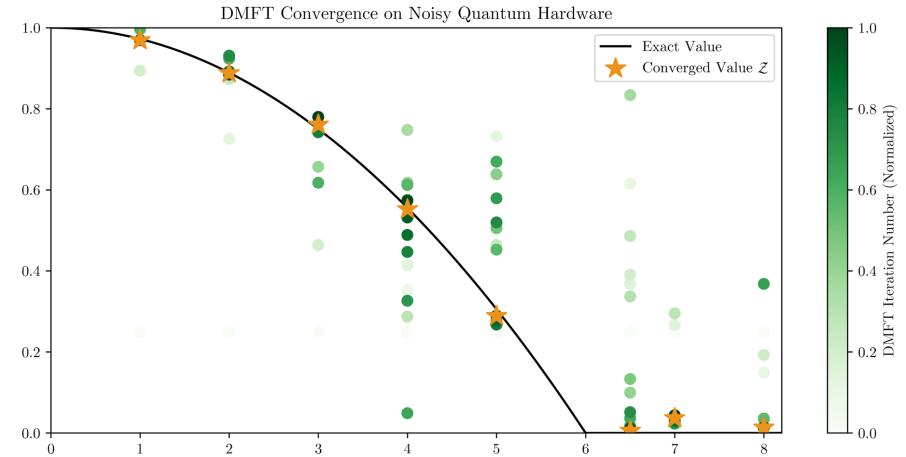


$$f(K) = \langle K v K^\dagger, \mathcal{H} \rangle$$

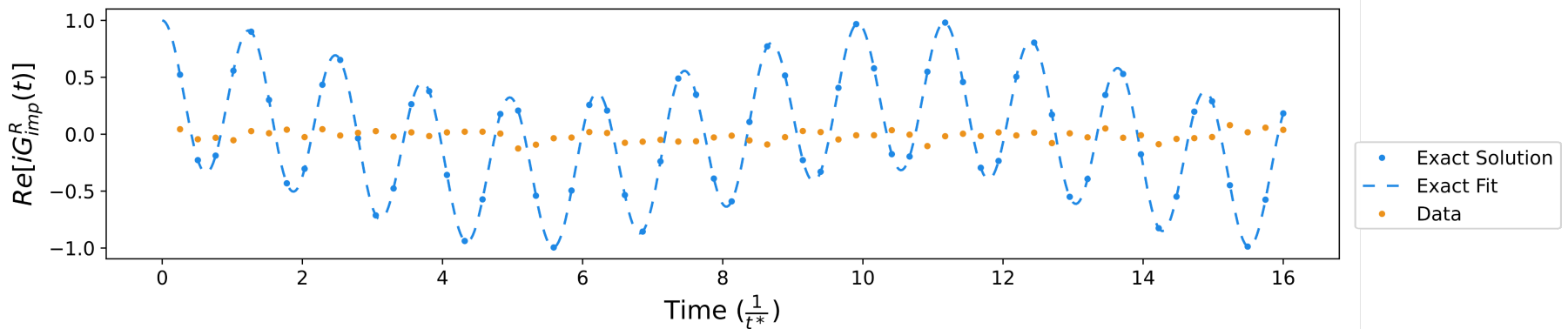


Cartan Decomposition

- $O(n^2)$ circuit for TFIM, TFX, XY
- Applicable for any model
- Optimize only once for any time t
- Obtained 1st ever self-consistent DMFT Hubbard phase diagram on IBM QC.

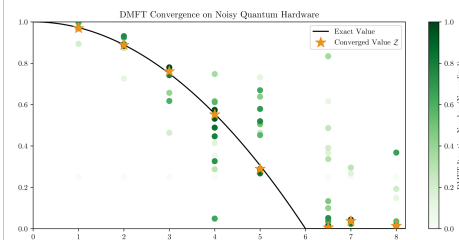
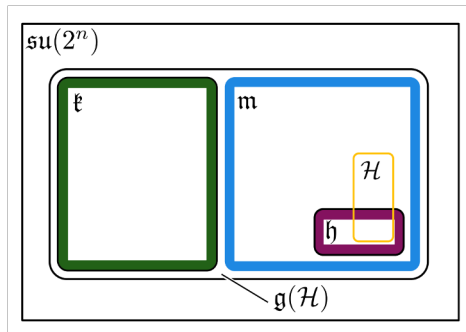


Cartan Based Simulation on IBM Lagos



2 Algebraic methods for circuit generation

Cartan Decomposition

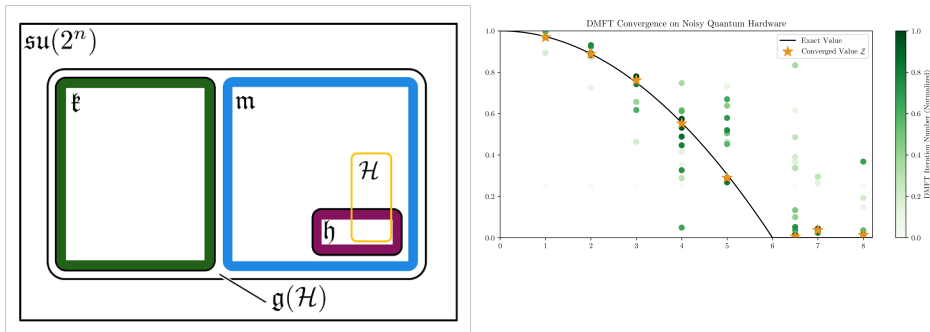


Algebraic Compression

- Produces exact, fixed depth time evolution unitaries for any model.
- Produces unitaries for linear combinations of (anti)-Hermitian operators (UCC factors).
- We have code available!
<https://github.com/kemperlab/cartan-quantum-synthesizer>

2 Algebraic methods for circuit generation

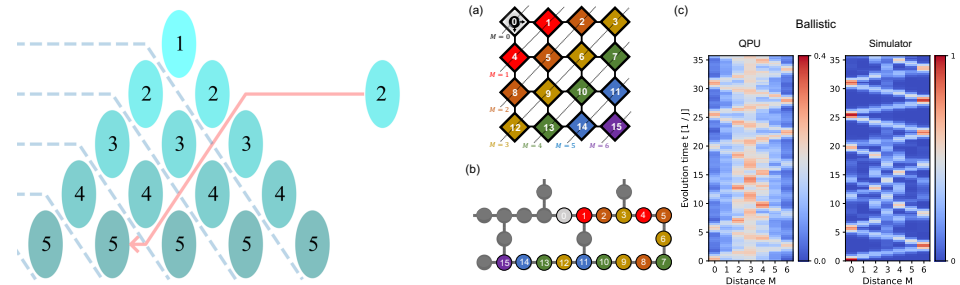
Cartan Decomposition



- Produces exact, fixed depth time evolution unitaries for any model.
- Produces unitaries for linear combinations of (anti)-Hermitian operators (UCC factors).
- We have code available!
<https://github.com/kemperlab/cartan-quantum-synthesizer>

Kökcü PRL (2022) , Steckmann PRR (2023)

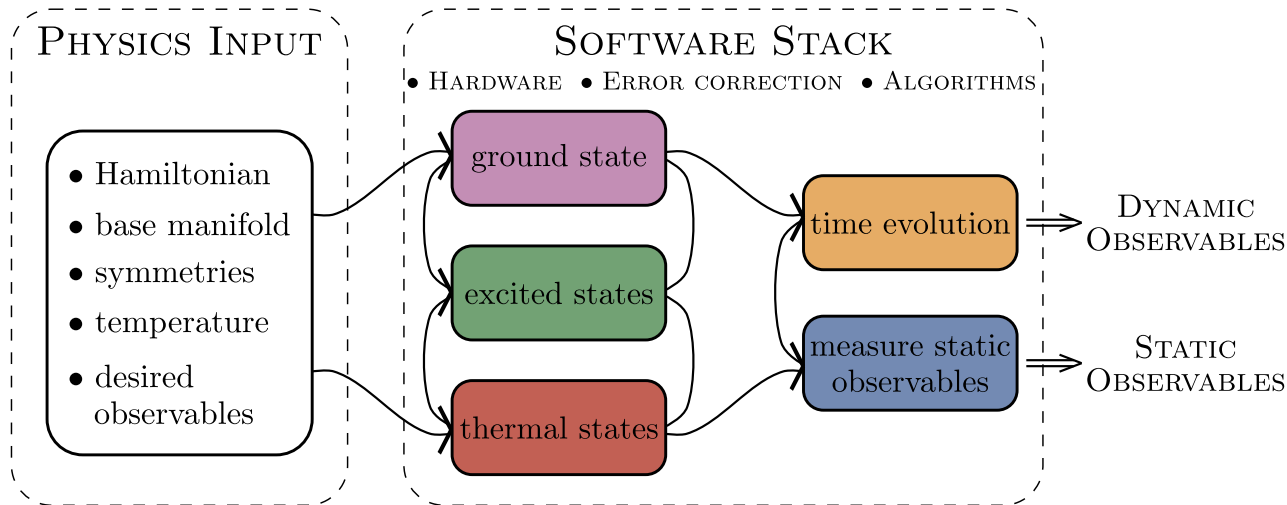
Algebraic Compression



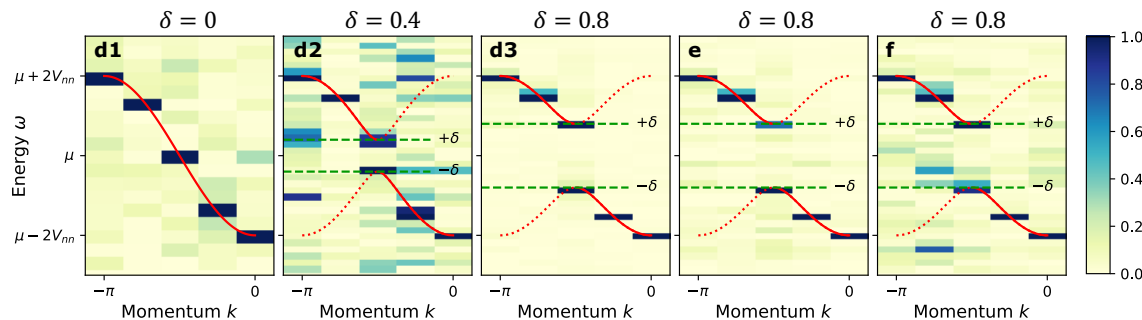
- Compressed Trotter circuits down to a shallow fixed depth circuit for 1-D nearest neighbor TFX, TFIM, XY and Kitaev models.
- Based on 3 easy to check, local properties.
- We have code available! Check F3C, F3C++ and F3Cpy at <https://github.com/QuantumComputingLab>

Kökcü PRA (2021), Camp SIMAX 2022, Kökcü arXiv:2303.09538

Quantum Matter meets Quantum Computing



<https://go.ncsu.edu/kemper-lab>



- Experimental relevance: Measuring correlation functions
- Measuring exact integer Chern numbers for topological states
- Open quantum evolution and fixed points (1000 Trotter steps)
- Time evolution via Lie algebraic decomposition and compression
- Thermodynamics via Lee-Yang Zeros
- Physics-Informed Subspace Expansions